May 28, 2003

RESPONSES TO QUESTIONS ON THE SAR REPORT FOR WISTRON NEWEB CORPORATION MODEL EM-500 AG802.11 a/b/g MINI PCI CARD BUILT INTO MODEL BQ12 NOTEBOOK COMPUTER

FCC ID# NKRBQ12AB
Host Computer: Model BQ12
SAR Report originally submitted: February 28, 2003

1. *Power measurement data for both before and after each scan.*

Response:

This is given in Tables a, b, where the measured peak 1-g SARs for each of the newly measured channels are summarized. Also included in these tables are the data previously submitted as Table 11 of the SAR report on this EUT dated February 28, 2003. The latter 1-g SARs for both the main and the auxiliary antennas are for the base mode at 5.26 GHz and for the turbo mode at 5.29 GHz. Because of fairly low average conducted powers for some of the channels, the SARs were too low to measure, within the noise limit of the SAR measurement system which is estimated to be 0.02 W/kg. As seen in Table a, this was especially true for the "Above-lap" Configuration 1 and may be due to the shielding effect of the base of the PC.

2. *Strong justification for system verification at 1.9 GHz (in the previously submitted SAR report dated February 28, 2003).*

Response:

Balanced dipoles were not available for use in the 5.1 to 5.8 GHz band and would have been very difficult to develop both because of fairly small physical dimensions and resulting dimensional tolerances, and relatively narrow bandwidths of the required baluns – balanced-to-unbalanced transformers. To alleviate this problem, we have proposed and recently developed an air-filled open-ended waveguide radiator for system validation. This system described in Appendix I has a simultaneous bandwidth of 1900 MHz which is far in excess of the required bandwidth of 700 MHz of the 5.1 to 5.8 GHz band. This system has been validated against FDTD-calculated peak 1-g SARs and has been used for all system validations in our laboratory after May 1, 2003.

The measured SAR distribution for peak 1-g SAR region using this system at 5.25 GHz for the day of the measurements May 22, 2003 is given in Appendix II. Also given in Appendix II are the waveguide SAR plots for this date of new SAR measurements. The peak 1-g SAR measured for 100 mW of radiated power at 5.25 GHz of 3.665 W/kg is in excellent agreement

with the FDTD-calculated SAR of 3.58 W/kg. Also as expected, the measured SAR plot in Appendix II is quite symmetric.

3. *New SAR plots to include date, temperatures, and probe and liquid factors.*

Response:

All of the new SAR plots and tables given here were obtained on May 22, 2003. The temperatures of the tissue-simulant fluid are given in Tables a and b. The probe calibration factor and liquid dielectric properties are the same as those given in the previous SAR test report submitted on February 28, 2003.

4. *Low, middle, and high channel SAR data consistent with Supplement C recommendations.*

Response:

The coarse scan SAR data for additional channels are given in Figs. a-j, respectively. The z-axis scan plots taken at the highest SAR locations for each set of tests are given in Figs. k, l, and m for Configurations 1 and 2, respectively. The detailed SAR distributions for the peak 1-g SAR regions are given in Tables c-l. From Tables a and b, it can be seen that all of the measured peak 1-g SARs varying from 0 to 0.909 W/kg are less than the FCC 96-326 Guideline of 1.6 W/kg.

5. *Demonstration that SAR remains constant for all transmitting modes/data rates.*

Response:

The stability of the conducted power/SAR was determined by repeated SAR measurements at the same location for each of the channels. The variability of the SAR thus determined for three repeated measurements over a 60-minute time period was within ± 2.5% (± 0.1 dB).

Table a. The peak 1-g SARs measured for the various channels for **Configuration 1** for Wistron Neweb Corporation 802.11a Wireless Antennas built into Model BQ12 Notebook PC (FCC ID# NKRBQ12AB). Also included are the data previously submitted as Table 11 of the SAR report dated February 28, 2003.

Configuration 1 – "Above-lap" position; bottom of PC pressed against bottom of the flat phantom – spacing to bottom of the phantom = 0 cm.

Frequency GHz	Antenna	Conducted Power (dBm)		Liquid Temperature °C	1-g SAR W/kg	For Detailed SAR Distribution See:	For Coarse Scan See:
		Before	After				
Base Mode							
5.18	Main Auxiliary	16.42 16.41	16.41 16.40	23.2 23.2	<0.02* <0.02*	---	---
5.26	Main Auxiliary	18.72 18.71	18.71 18.70	23.2 23.2	0.223 0.164	Prev. rept.[1] Prev. rept.	Prev. rept. Prev. rept.
5.32	Main Auxiliary	18.22 18.20	18.21 18.16	23.2 23.2	0.126 0.092	Table c Table d	Fig. a Fig. b
Turbo Mode							
5.21	Main Auxiliary	16.25 16.24	16.23 16.22	23.3 23.2	<0.02* <0.02*	---	---
5.25	Main Auxiliary	16.37 16.34	16.35 16.33	23.2 23.2	<0.02* <0.02*	---	---
5.29	Main Auxiliary	17.48 17.42	17.42 17.39	23.3 23.2	0.206 0.125	Prev. rept. Prev. rept.	Prev. rept. Prev. rept.

* Too low to measure, within the noise limit of the SAR measurement system.
[1] Previous report submitted February 28, 2003.

Table b. The peak 1-g SARs measured for the various channels for **Configuration 2** for Wistron Neweb Corporation 802.11a Wireless Antennas built into Model BQ12 Notebook PC (FCC ID# NKRBQ12AB). Also included are the data previously submitted as Table 11 of the SAR report dated February 28, 2003.

Configuration 2 – "Edge-on" placement; right or left edge of the PC at 90° and a distance of 1.5 cm from the base of the phantom – spacing to bottom of the phantom = 1.5 cm.

Frequency GHz	Antenna	Conducted Power (dBm)		Liquid Temperature °C	1-g SAR W/kg	For Detailed SAR Distribution See:	For Coarse Scan See:
		Before	After				
Base Mode							
5.18	Main	16.42	16.41	23.2	0.363	Table e	Fig. c
	Auxiliary	16.41	16.40	23.2	0.547	Table f	Fig. d
5.26	Main	18.72	18.71	23.3	0.699	Prev. rept.[1]	Prev. rept.
	Auxiliary	18.71	18.70	23.2	0.909	Prev. rept.	Prev. rept.
5.32	Main	18.22	18.21	23.2	0.595	Table g	Fig. e
	Auxiliary	18.20	18.16	23.2	0.686	Table h	Fig. f
Turbo Mode							
5.21	Main	16.25	16.23	23.2	0.351	Table i	Fig. g
	Auxiliary	16.21	16.22	23.2	0.495	Table j	Fig. h
5.25	Main	16.37	16.35	23.2	0.351	Table k	Fig. i
	Auxiliary	16.34	16.33	23.2	0.503	Table l	Fig. j
5.29	Main	17.48	17.42	23.3	0.613	Prev. rept.	Prev. rept.
	Auxiliary	17.42	17.39	23.2	0.597	Prev. rept.	Prev. rept.

[1] Previous report submitted February 28, 2003.

Table c. **Above-lap position (Configuration 1).** The SARs measured for the Wistron Neweb Model BQ12 802.11a **Main** Wireless Antenna for the base mode at 5.32 GHz**.**

1-g SAR = 0.126 W/kg

a. At depth of 1 mm

0.203	0.162	0.100	0.140	0.191
0.142	0.046	0.144	0.173	0.220
0.247	0.221	0.121	0.148	0.145
0.229	0.247	0.154	0.208	0.248
0.206	0.210	0.332	0.271	0.352

b. At depth of 3 mm

0.132	0.104	0.138	0.124	0.130
0.119	0.120	0.119	0.119	0.135
0.161	0.131	0.122	0.130	0.118
0.140	0.156	0.115	0.135	0.157
0.146	0.141	0.168	0.183	0.210

c. At depth of 5 mm

0.101	0.087	0.132	0.102	0.097
0.105	0.127	0.105	0.098	0.095
0.124	0.095	0.103	0.110	0.105
0.105	0.112	0.096	0.104	0.120
0.109	0.106	0.109	0.146	0.157

d. At depth of 7 mm

0.089	0.088	0.110	0.083	0.082
0.095	0.105	0.098	0.089	0.081
0.108	0.085	0.085	0.092	0.096
0.093	0.096	0.085	0.095	0.106
0.090	0.092	0.098	0.135	0.144

e. At depth of 9 mm

0.084	0.092	0.091	0.071	0.075
0.089	0.083	0.095	0.081	0.078
0.097	0.082	0.079	0.078	0.085
0.085	0.091	0.079	0.094	0.096
0.083	0.089	0.099	0.134	0.140

Table d. **Above-lap position (Configuration 1).** The SARs measured for the Wistron Neweb Model BQ12 802.11a **Auxiliary** Wireless Antenna for the base mode at 5.32 GHz**.**

1-g SAR = 0.092 W/kg

a. At depth of 1 mm

0.082	0.139	0.202	0.118	0.283
0.265	0.207	0.212	0.180	0.075
0.098	0.100	0.262	0.169	0.351
0.095	0.065	0.043	0.050	0.159
0.122	0.090	0.103	0.203	0.201

b. At depth of 3 mm

0.069	0.107	0.126	0.112	0.146
0.127	0.118	0.108	0.114	0.078
0.092	0.077	0.119	0.129	0.170
0.094	0.069	0.051	0.081	0.086
0.081	0.089	0.068	0.127	0.154

c. At depth of 5 mm

0.062	0.087	0.090	0.095	0.090
0.073	0.070	0.065	0.072	0.079
0.078	0.064	0.068	0.095	0.099
0.086	0.062	0.049	0.079	0.051
0.071	0.077	0.057	0.104	0.132

d. At depth of 7 mm

0.059	0.070	0.074	0.077	0.072
0.059	0.046	0.052	0.048	0.074
0.064	0.057	0.058	0.073	0.077
0.073	0.051	0.045	0.066	0.037
0.069	0.066	0.055	0.100	0.124

e. At depth of 9 mm

0.057	0.051	0.066	0.063	0.064
0.059	0.034	0.049	0.037	0.063
0.052	0.051	0.056	0.062	0.067
0.060	0.041	0.043	0.054	0.033
0.062	0.060	0.055	0.097	0.121

Table e. **Edge-on position (Configuration 2).** The SARs measured for the Wistron Neweb Model BQ12 802.11a **Main** Wireless Antenna for the base mode at 5.18 GHz**.**

1-g SAR = 0.363 W/kg

a. At depth of 1 mm

0.657	0.501	0.705	0.852	0.502
0.826	0.875	0.913	0.673	0.737
0.756	0.938	0.757	0.815	0.431
0.871	0.913	0.864	0.760	0.796
0.758	0.805	0.855	0.649	0.826

b. At depth of 3 mm

0.401	0.376	0.398	0.421	0.352
0.451	0.462	0.463	0.427	0.408
0.424	0.481	0.455	0.443	0.352
0.452	0.463	0.463	0.416	0.405
0.432	0.449	0.462	0.426	0.433

c. At depth of 5 mm

0.244	0.258	0.249	0.233	0.246
0.274	0.268	0.266	0.282	0.252
0.249	0.275	0.288	0.263	0.257
0.260	0.267	0.273	0.252	0.246
0.275	0.285	0.287	0.291	0.269

d. At depth of 7 mm

0.164	0.173	0.184	0.171	0.181
0.202	0.192	0.195	0.204	0.188
0.172	0.199	0.204	0.188	0.177
0.189	0.200	0.199	0.186	0.199
0.210	0.224	0.222	0.219	0.213

e. At depth of 9 mm

0.134	0.130	0.154	0.155	0.150
0.170	0.162	0.166	0.165	0.159
0.146	0.171	0.165	0.158	0.128
0.167	0.179	0.171	0.160	0.182
0.182	0.205	0.197	0.190	0.189

Table f. **Edge-on position (Configuration 2).** The SARs measured for the Wistron Neweb Model BQ12 802.11a **Auxiliary** Wireless Antenna for the base mode at 5.18 GHz**.**

1-g SAR = 0.547 W/kg

a. At depth of 1 mm

1.105	1.348	1.131	1.301	1.104
0.828	1.308	1.215	1.251	1.297
1.195	1.352	1.405	1.104	0.948
1.281	1.274	1.104	1.154	1.061
1.090	1.044	0.974	0.969	1.028

b. At depth of 3 mm

0.632	0.713	0.659	0.646	0.592
0.597	0.692	0.665	0.659	0.650
0.688	0.711	0.702	0.618	0.564
0.675	0.676	0.663	0.645	0.582
0.652	0.628	0.621	0.588	0.586

c. At depth of 5 mm

0.393	0.416	0.408	0.368	0.354
0.410	0.412	0.394	0.384	0.373
0.424	0.410	0.385	0.386	0.367
0.396	0.393	0.410	0.397	0.366
0.418	0.416	0.427	0.395	0.377

d. At depth of 7 mm

0.289	0.297	0.291	0.277	0.263
0.285	0.307	0.277	0.276	0.281
0.302	0.292	0.274	0.289	0.276
0.290	0.282	0.283	0.294	0.288
0.307	0.318	0.328	0.307	0.293

e. At depth of 9 mm

0.246	0.251	0.241	0.250	0.229
0.226	0.266	0.229	0.234	0.252
0.249	0.247	0.242	0.247	0.233
0.250	0.246	0.231	0.253	0.260
0.261	0.272	0.277	0.266	0.263

Table g. **Edge-on position (Configuration 2).** The SARs measured for the Wistron Neweb Model BQ12 802.11a **Main** Wireless Antenna for the base mode at 5.32 GHz**.**

1-g SAR = 0.595 W/kg

a. At depth of 1 mm

1.398	1.303	1.444	1.359	1.419
1.458	1.683	1.505	1.657	1.320
1.539	1.677	1.505	1.580	1.697
1.471	1.586	1.594	1.452	1.483
1.346	1.252	1.530	1.654	1.476

b. At depth of 3 mm

0.690	0.683	0.707	0.675	0.639
0.721	0.777	0.743	0.762	0.666
0.757	0.789	0.788	0.770	0.761
0.716	0.762	0.795	0.765	0.736
0.675	0.707	0.777	0.789	0.763

c. At depth of 5 mm

0.344	0.343	0.353	0.338	0.289
0.359	0.358	0.368	0.350	0.333
0.385	0.374	0.413	0.384	0.355
0.355	0.380	0.403	0.407	0.374
0.341	0.393	0.406	0.401	0.420

d. At depth of 7 mm

0.198	0.181	0.206	0.192	0.163
0.205	0.200	0.211	0.192	0.186
0.231	0.213	0.238	0.226	0.213
0.210	0.230	0.238	0.242	0.223
0.201	0.233	0.250	0.257	0.281

e. At depth of 9 mm

0.139	0.115	0.146	0.131	0.121
0.143	0.149	0.151	0.135	0.130
0.167	0.156	0.162	0.161	0.159
0.157	0.170	0.172	0.170	0.163
0.151	0.164	0.193	0.201	0.230

Table h. **Edge-on position (Configuration 2).** The SARs measured for the Wistron Neweb Model BQ12 802.11a **Auxiliary** Wireless Antenna for the base mode at 5.32 GHz**.**

1-g SAR = 0.686 W/kg

a. At depth of 1 mm

1.548	1.551	1.498	1.372	1.293
1.547	1.631	1.760	1.484	1.512
1.621	1.762	1.477	1.757	1.555
1.658	1.509	1.573	1.546	1.365
1.459	1.594	1.580	1.394	1.420

b. At depth of 3 mm

0.789	0.821	0.808	0.755	0.704
0.828	0.864	0.888	0.806	0.770
0.864	0.903	0.824	0.864	0.811
0.882	0.859	0.861	0.850	0.744
0.813	0.856	0.852	0.796	0.759

c. At depth of 5 mm

0.444	0.460	0.468	0.449	0.419
0.474	0.484	0.478	0.459	0.434
0.487	0.493	0.486	0.463	0.463
0.513	0.497	0.500	0.491	0.438
0.485	0.503	0.501	0.483	0.452

d. At depth of 7 mm

0.310	0.310	0.326	0.316	0.299
0.324	0.322	0.319	0.307	0.310
0.325	0.329	0.329	0.318	0.325
0.361	0.323	0.340	0.332	0.311
0.339	0.356	0.354	0.338	0.329

e. At depth of 9 mm

0.254	0.254	0.272	0.262	0.249
0.265	0.262	0.262	0.250	0.264
0.260	0.270	0.256	0.267	0.271
0.297	0.254	0.274	0.271	0.263
0.279	0.295	0.292	0.277	0.278

Table i. **Edge-on position (Configuration 2).** The SARs measured for the Wistron Neweb Model BQ12 802.11a **Main** Wireless Antenna for the turbo mode at 5.21 GHz**.**

1-g SAR = 0.351 W/kg

a. At depth of 1 mm

0.945	0.923	0.743	0.851	0.672
0.773	0.763	1.000	0.916	0.791
0.765	0.946	0.853	0.910	0.765
1.002	0.859	0.814	0.876	0.814
0.578	0.781	0.959	0.652	0.909

b. At depth of 3 mm

0.446	0.446	0.382	0.406	0.349
0.406	0.423	0.445	0.437	0.394
0.417	0.457	0.433	0.437	0.414
0.458	0.447	0.447	0.427	0.435
0.354	0.408	0.454	0.401	0.456

c. At depth of 5 mm

0.237	0.226	0.211	0.212	0.196
0.220	0.236	0.218	0.215	0.209
0.233	0.224	0.227	0.224	0.232
0.226	0.248	0.252	0.227	0.252
0.220	0.223	0.231	0.262	0.250

d. At depth of 7 mm

0.168	0.145	0.139	0.145	0.131
0.140	0.144	0.148	0.134	0.135
0.148	0.131	0.139	0.144	0.145
0.149	0.164	0.157	0.156	0.173
0.150	0.146	0.155	0.191	0.175

e. At depth of 9 mm

0.142	0.120	0.105	0.122	0.101
0.108	0.106	0.126	0.110	0.104
0.112	0.098	0.105	0.111	0.104
0.121	0.128	0.114	0.133	0.134
0.121	0.116	0.132	0.153	0.152

Table j. **Edge-on position (Configuration 2).** The SARs measured for the Wistron Neweb Model BQ12 802.11a **Auxiliary** Wireless Antenna for the turbo mode at 5.21 GHz**.**

1-g SAR = 0.495 W/kg

a. At depth of 1 mm

1.176	1.261	1.107	1.107	1.076
1.101	1.162	1.325	1.194	1.107
1.037	1.157	1.078	1.264	1.173
0.851	0.835	0.934	1.003	0.845
0.864	0.945	1.058	0.811	0.907

b. At depth of 3 mm

0.594	0.648	0.621	0.630	0.595
0.583	0.622	0.683	0.662	0.610
0.554	0.609	0.615	0.639	0.610
0.506	0.522	0.576	0.561	0.507
0.504	0.549	0.574	0.546	0.542

c. At depth of 5 mm

0.342	0.369	0.366	0.374	0.351
0.341	0.368	0.385	0.390	0.356
0.329	0.363	0.380	0.351	0.346
0.320	0.345	0.370	0.347	0.331
0.324	0.352	0.352	0.385	0.381

d. At depth of 7 mm

0.255	0.263	0.249	0.255	0.244
0.246	0.265	0.269	0.270	0.246
0.241	0.265	0.276	0.241	0.242
0.232	0.249	0.262	0.256	0.248
0.246	0.268	0.270	0.295	0.320

e. At depth of 9 mm

0.223	0.220	0.203	0.207	0.201
0.211	0.222	0.224	0.220	0.204
0.207	0.219	0.229	0.201	0.202
0.198	0.194	0.213	0.215	0.207
0.213	0.234	0.245	0.251	0.290

Table k. **Edge-on position (Configuration 2).** The SARs measured for the Wistron Neweb Model BQ12 802.11a **Main** Wireless Antenna for the turbo mode at 5.25 GHz**.**

1-g SAR = 0.351 W/kg

a. At depth of 1 mm

0.822	0.790	0.594	0.654	0.601
0.731	0.836	0.882	0.589	0.573
0.615	0.711	0.556	0.791	0.835
0.598	0.647	0.653	0.678	0.617
0.715	0.827	0.635	0.596	0.699

b. At depth of 3 mm

0.435	0.438	0.395	0.395	0.366
0.438	0.474	0.477	0.415	0.387
0.400	0.434	0.405	0.464	0.400
0.402	0.433	0.420	0.384	0.376
0.401	0.436	0.410	0.435	0.432

c. At depth of 5 mm

0.262	0.272	0.276	0.264	0.253
0.291	0.305	0.283	0.305	0.268
0.266	0.283	0.288	0.296	0.218
0.274	0.253	0.278	0.245	0.254
0.244	0.254	0.273	0.297	0.293

d. At depth of 7 mm

0.201	0.206	0.209	0.208	0.206
0.225	0.238	0.203	0.240	0.200
0.197	0.207	0.215	0.220	0.164
0.201	0.143	0.204	0.188	0.194
0.176	0.180	0.201	0.207	0.223

e. At depth of 9 mm

0.180	0.181	0.172	0.186	0.186
0.195	0.210	0.173	0.203	0.167
0.170	0.167	0.183	0.186	0.153
0.165	0.109	0.175	0.164	0.156
0.150	0.145	0.171	0.172	0.184

Table l. **Edge-on position (Configuration 2).** The SARs measured for the Wistron Neweb Model BQ12 802.11a **Auxiliary**Wireless Antenna for the turbo mode at 5.25GHz**.**

1-g SAR = 0.503 W/kg

a. At depth of 1 mm

0.871	0.929	1.081	1.018	0.694
0.911	1.119	1.160	1.076	0.955
0.993	0.969	1.082	1.104	1.216
0.992	1.212	1.020	1.376	1.213
0.953	1.046	1.204	1.119	0.850

b. At depth of 3 mm

0.489	0.520	0.558	0.572	0.484
0.535	0.608	0.626	0.586	0.564
0.549	0.581	0.632	0.622	0.614
0.574	0.631	0.619	0.685	0.635
0.563	0.593	0.656	0.654	0.604

c. At depth of 5 mm

0.310	0.328	0.332	0.363	0.344
0.346	0.371	0.382	0.359	0.357
0.349	0.378	0.383	0.374	0.344
0.372	0.373	0.400	0.384	0.374
0.360	0.380	0.400	0.420	0.429

d. At depth of 7 mm

0.239	0.250	0.252	0.280	0.261
0.260	0.282	0.285	0.270	0.259
0.271	0.283	0.264	0.264	0.248
0.285	0.282	0.291	0.280	0.276
0.267	0.291	0.302	0.319	0.318

e. At depth of 9 mm

0.212	0.216	0.223	0.245	0.221
0.219	0.251	0.243	0.235	0.216
0.237	0.243	0.220	0.218	0.220
0.247	0.249	0.238	0.244	0.238
0.229	0.252	0.271	0.283	0.258

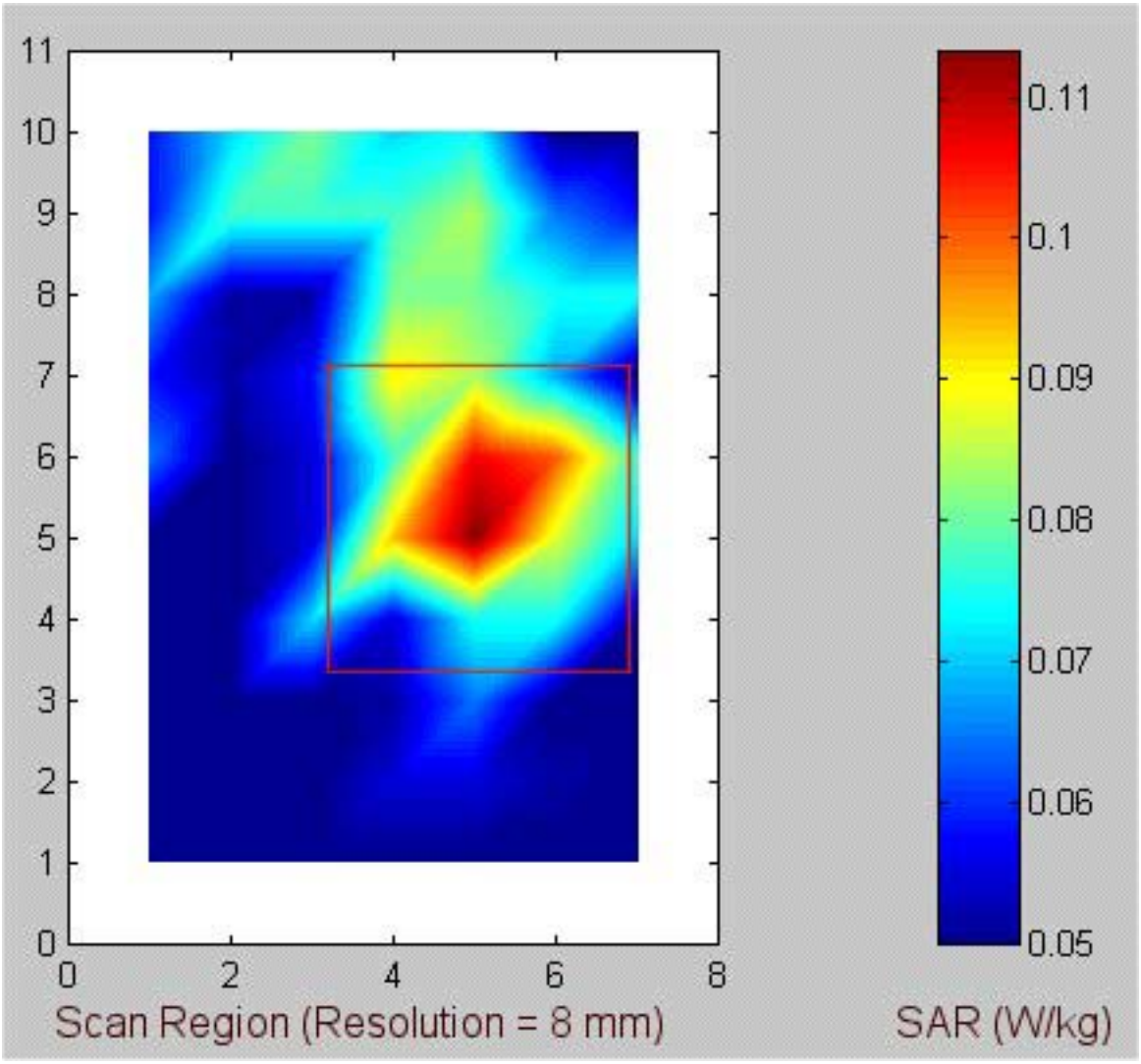

5.32 GHz **Base** mode – **Main** antenna (see Table c for peak 1-g SAR).

Fig. a. Coarse scans for the SAR measurements for the **Above-lap** position of the PC relative to the flat phantom (Configuration 1, see Fig. 3 of the previously submitted SAR report dated February 28, 2003). The base of the right or left sides of the PC with Main or Auxiliary 802.11a antennas, respectively, was placed pressed against the bottom of the flat phantom.

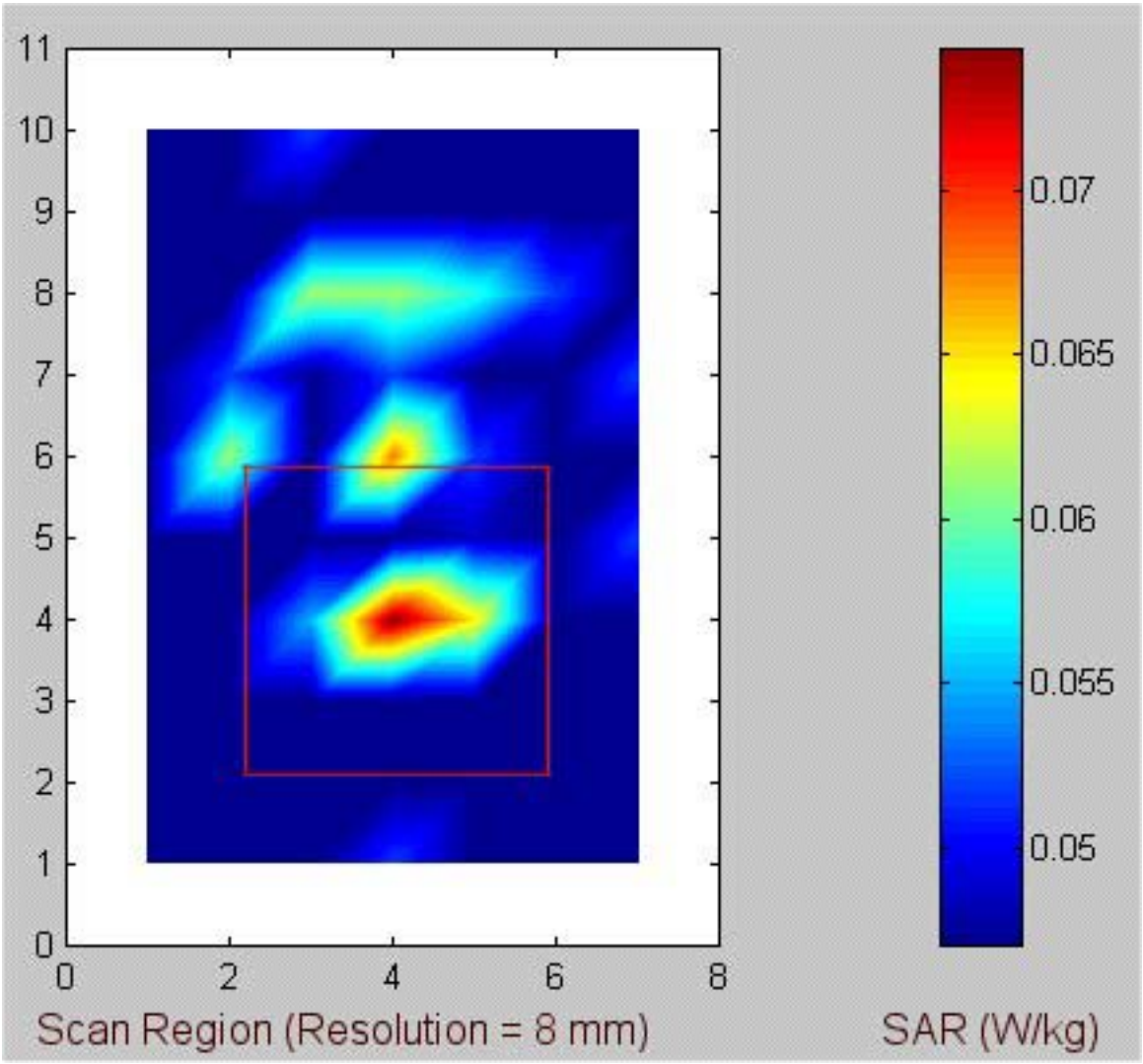

5.32 GHz **Base** mode – **Auxiliary** antenna (see Table d for peak 1-g SAR).

Fig. b. Coarse scans for the SAR measurements for the **Above-lap** position of the PC relative to the flat phantom (Configuration 1, see Fig. 3 of the previously submitted SAR report dated February 28, 2003). The base of the right or left sides of the PC with Main or Auxiliary 802.11a antennas, respectively, was placed pressed against the bottom of the flat phantom.

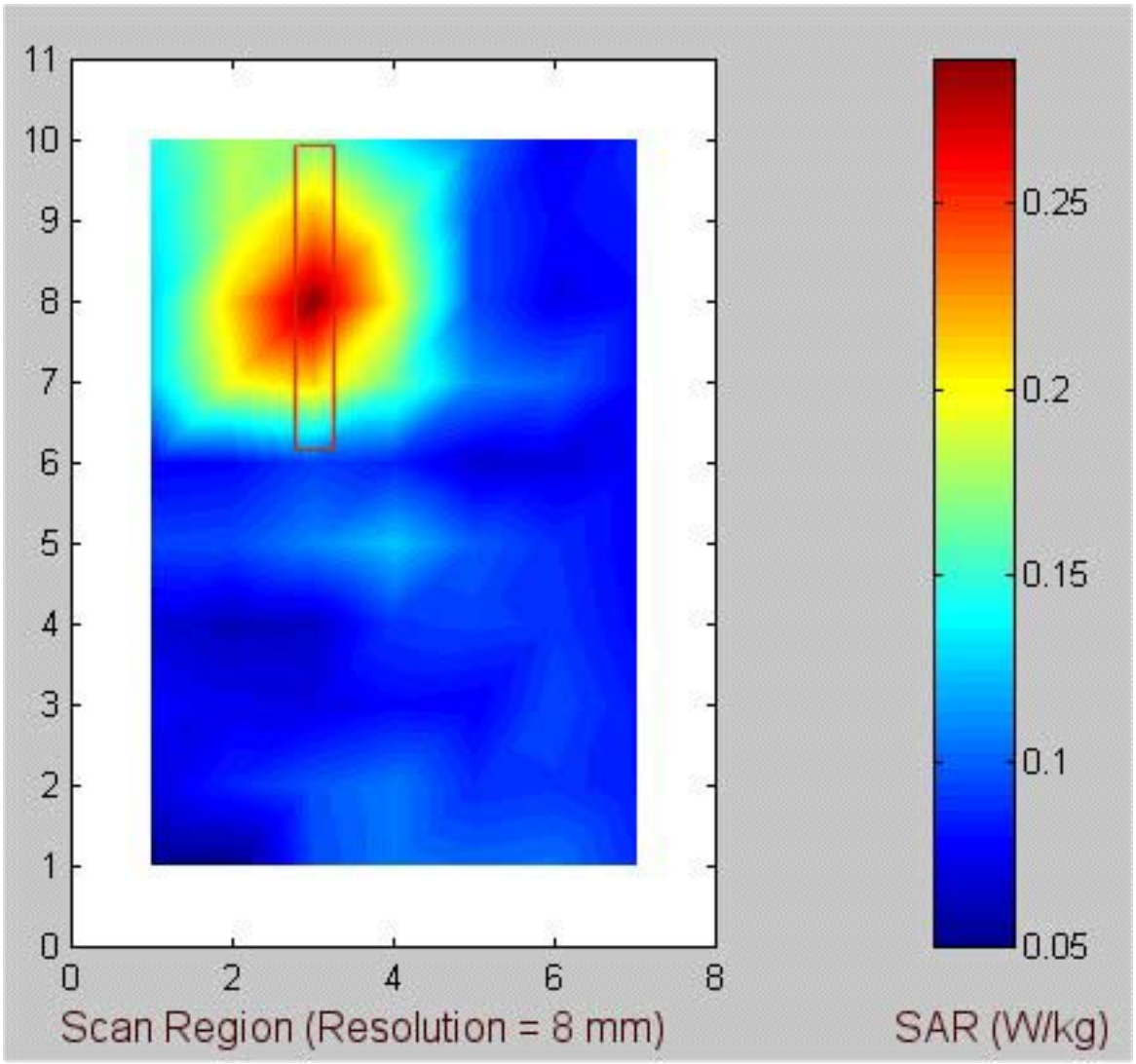

5.18 GHz **Base** mode – **Main** antenna (see Table e for peak 1-g SAR).

Fig. c. Coarse scans for the SAR measurements for the **Edge-on** position of the PC relative to the flat phantom (Configuration 2, see Fig. 4 of the previously submitted SAR report dated February 28, 2003). The right or left edge of the PC with 802.11a Main or Auxiliary antennas, respectively, was placed at 90° at a distance of 1.5 cm from the bottom of the flat phantom.

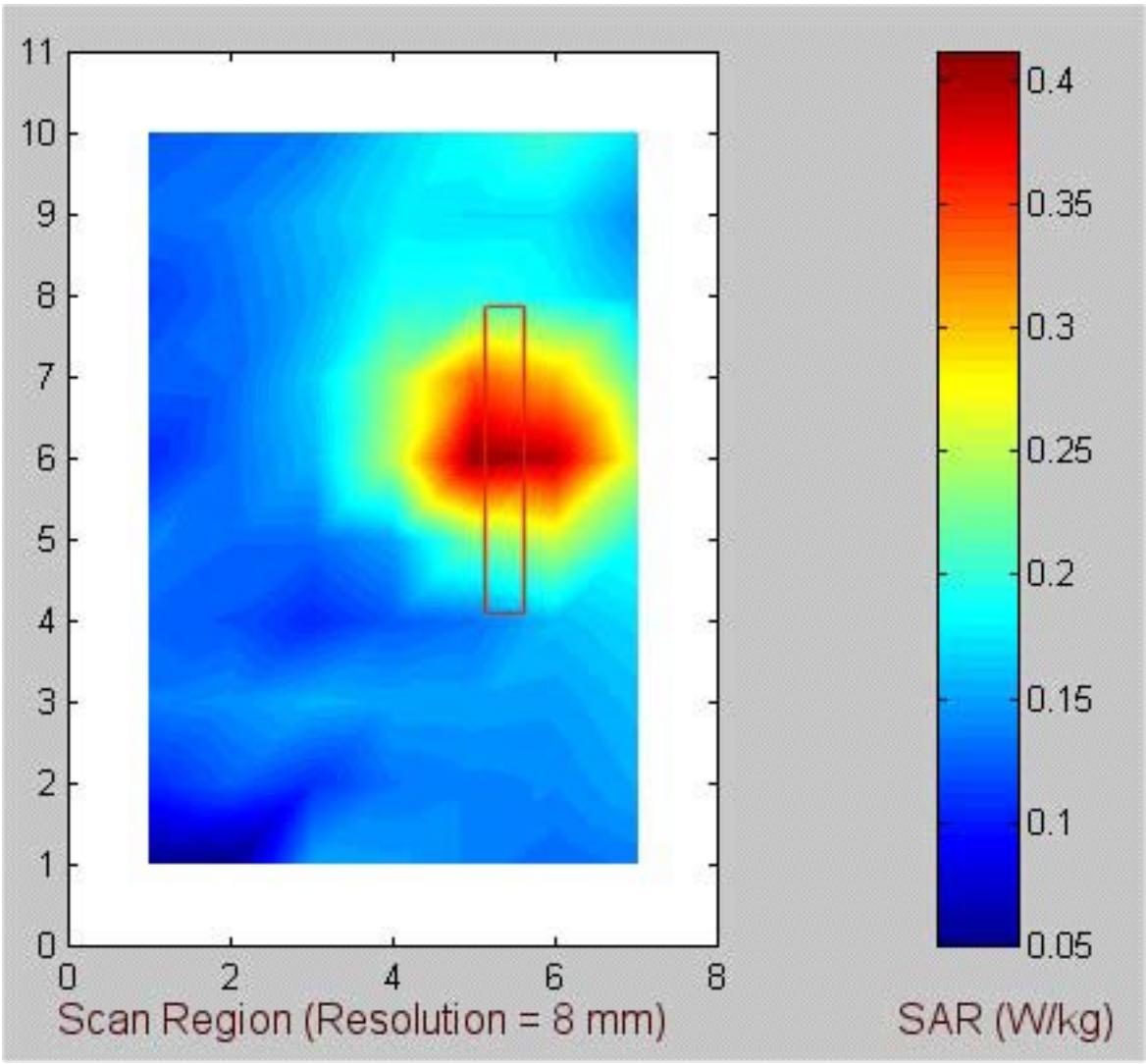

5.18 GHz **Base** mode – **Auxiliary** antenna (see Table f for peak 1-g SAR).

Fig. d. Coarse scans for the SAR measurements for the **Edge-on** position of the PC relative to the flat phantom (Configuration 2, see Fig. 4 of the previously submitted SAR report dated February 28, 2003). The right or left edge of the PC with 802.11a Main or Auxiliary antennas, respectively, was placed at 90° at a distance of 1.5 cm from the bottom of the flat phantom.

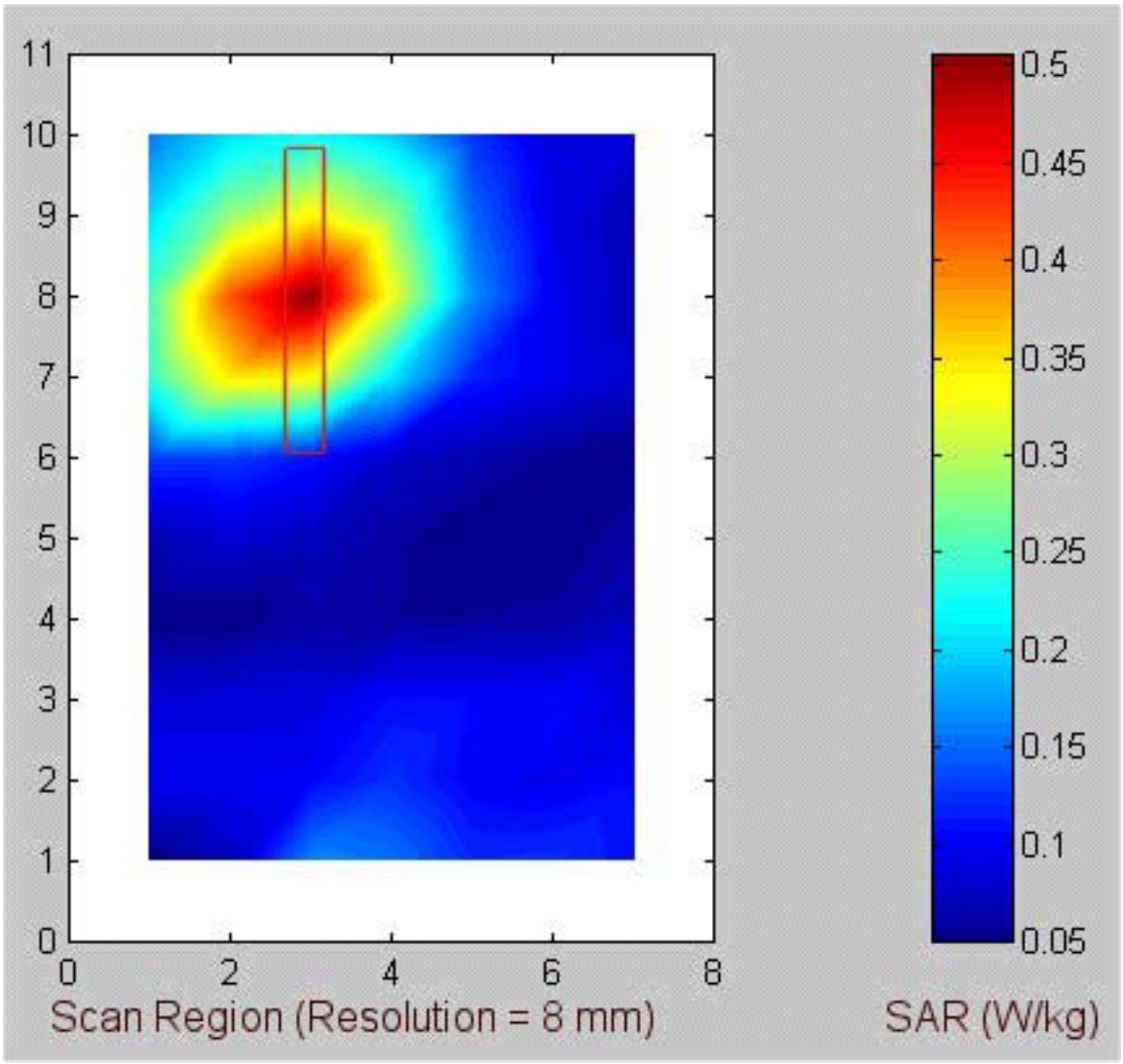

5.32 GHz **Base** mode – **Main** antenna (see Table g for peak 1-g SAR).

Fig. e. Coarse scans for the SAR measurements for the **Edge-on** position of the PC relative to the flat phantom (Configuration 2, see Fig. 4 of the previously submitted SAR report dated February 28, 2003). The right or left edge of the PC with 802.11a Main or Auxiliary antennas, respectively, was placed at 90° at a distance of 1.5 cm from the bottom of the flat phantom.

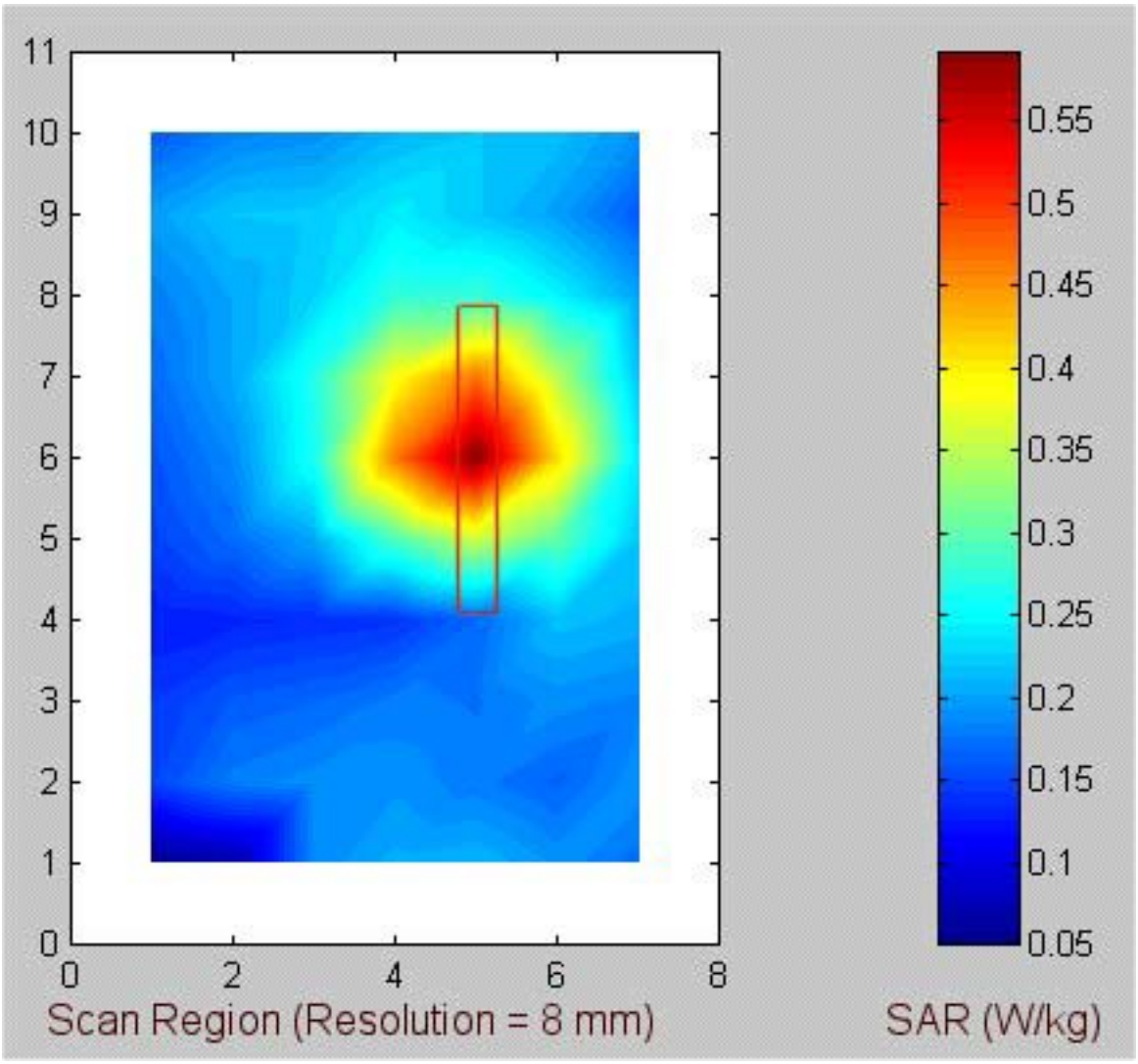

5.32 GHz **Base** mode – **Auxiliary** antenna (see Table h for peak 1-g SAR).

Fig. f. Coarse scans for the SAR measurements for the **Edge-on** position of the PC relative to the flat phantom (Configuration 2, see Fig. 4 of the previously submitted SAR report dated February 28, 2003). The right or left edge of the PC with 802.11a Main or Auxiliary antennas, respectively, was placed at 90° at a distance of 1.5 cm from the bottom of the flat phantom.

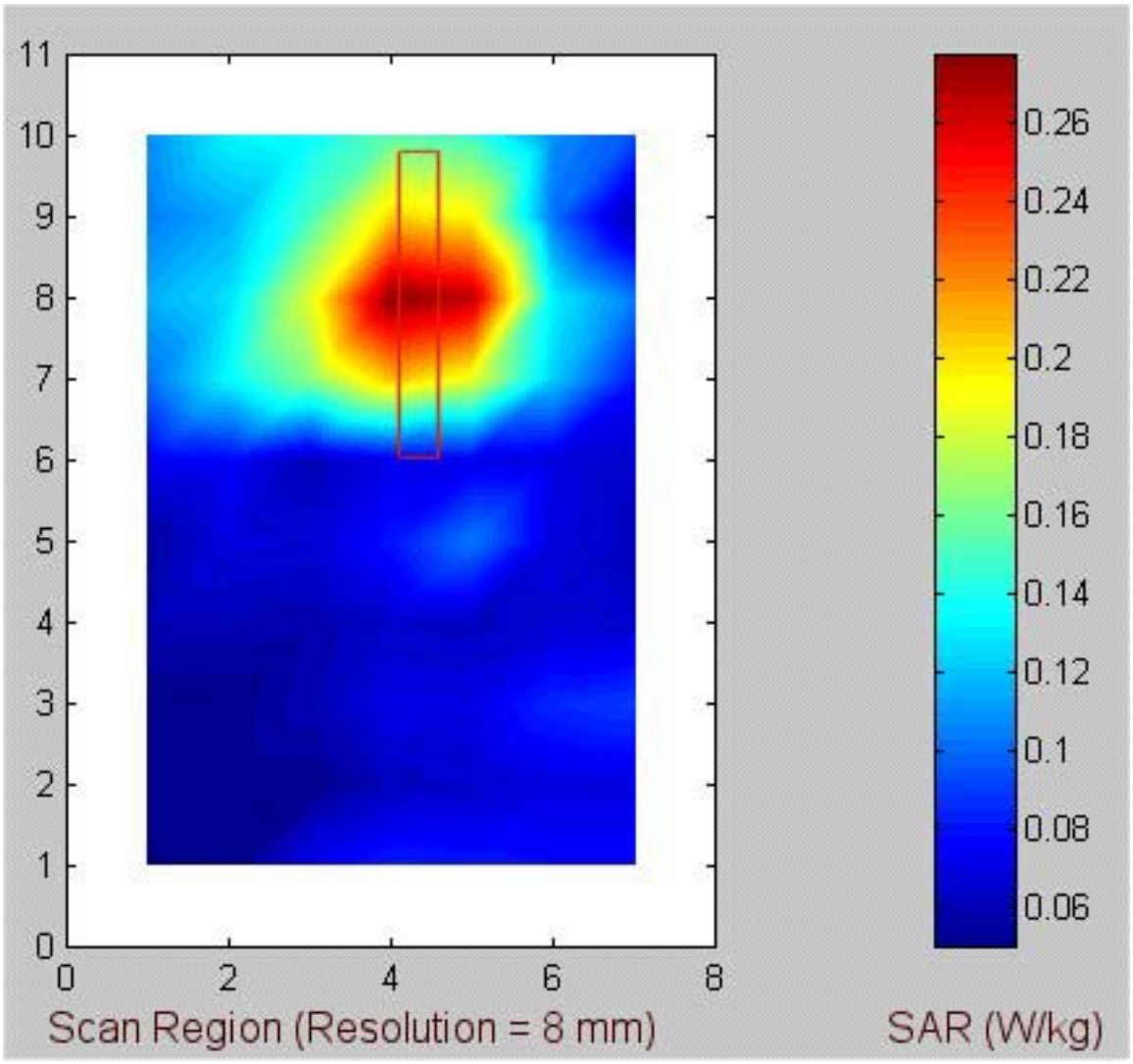

5.21 GHz **Turbo** mode – **Main** antenna (see Table i for peak 1-g SAR).

Fig. g. Coarse scans for the SAR measurements for the **Edge-on** position of the PC relative to the flat phantom (Configuration 2, see Fig. 4 of the previously submitted SAR report dated February 28, 2003). The right or left edge of the PC with 802.11a Main or Auxiliary antennas, respectively, was placed at 90° at a distance of 1.5 cm from the bottom of the flat phantom.

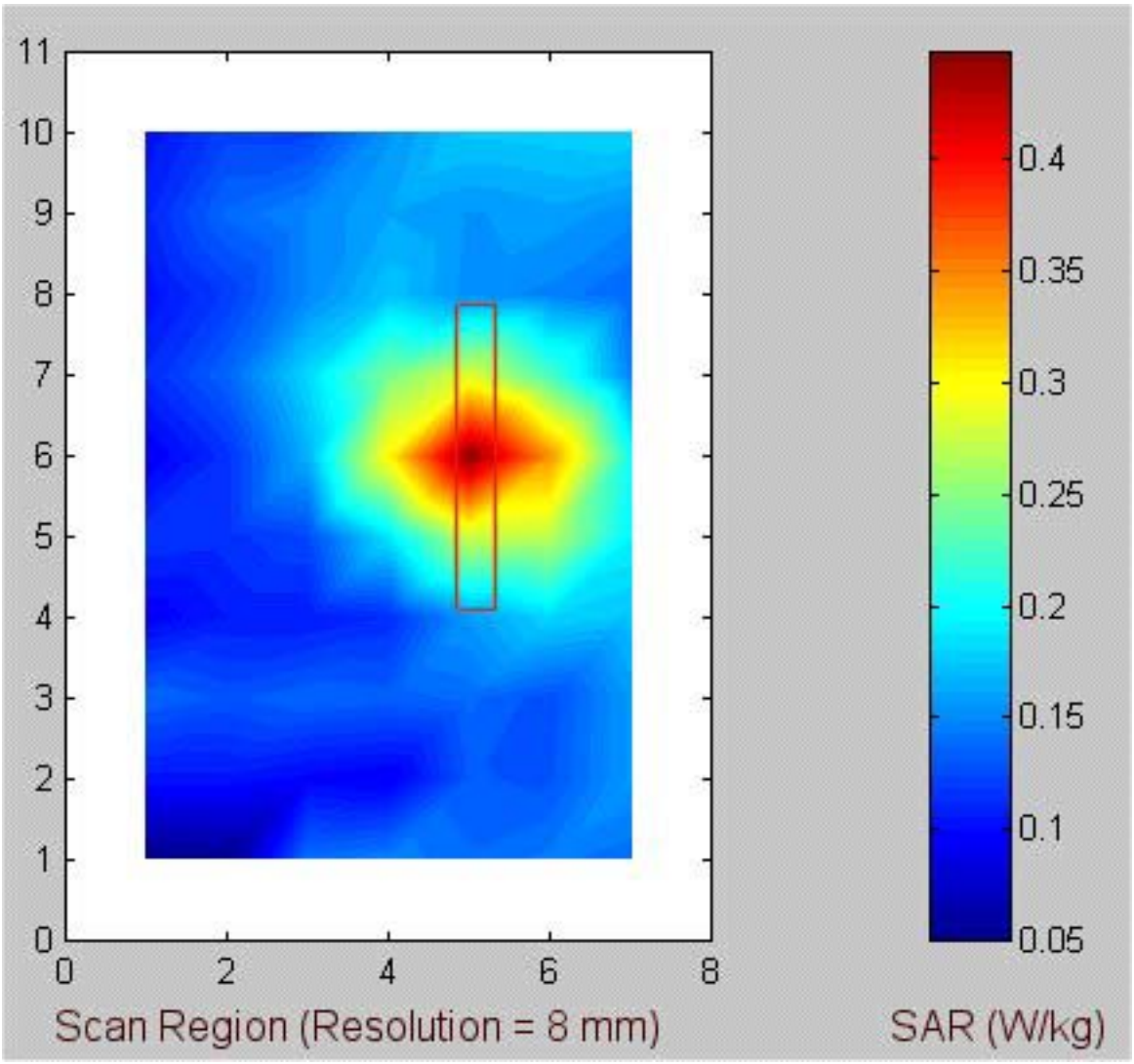

5.21 GHz **Turbo** mode – **Auxiliary** antenna (see Table j for peak 1-g SAR).

Fig. h. Coarse scans for the SAR measurements for the **Edge-on** position of the PC relative to the flat phantom (Configuration 2, see Fig. 4 of the previously submitted SAR report dated February 28, 2003). The right or left edge of the PC with 802.11a Main or Auxiliary antennas, respectively, was placed at 90° at a distance of 1.5 cm from the bottom of the flat phantom.

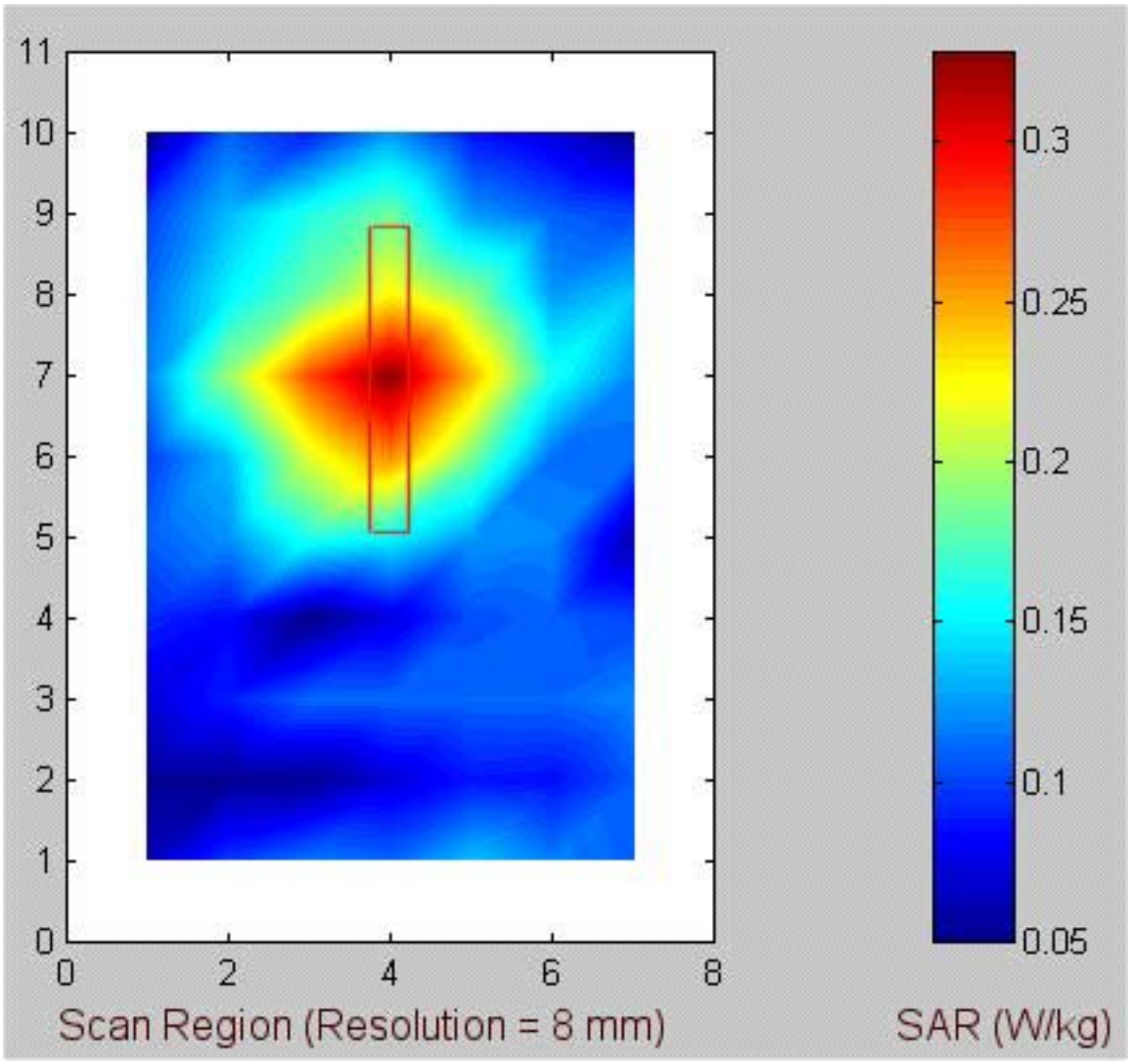

5.25 GHz **Turbo** mode – **Main** antenna (see Table k for peak 1-g SAR).

Fig. i. Coarse scans for the SAR measurements for the **Edge-on** position of the PC relative to the flat phantom (Configuration 2, see Fig. 4 of the previously submitted SAR report dated February 28, 2003). The right or left edge of the PC with 802.11a Main or Auxiliary antennas, respectively, was placed at 90° at a distance of 1.5 cm from the bottom of the flat phantom.

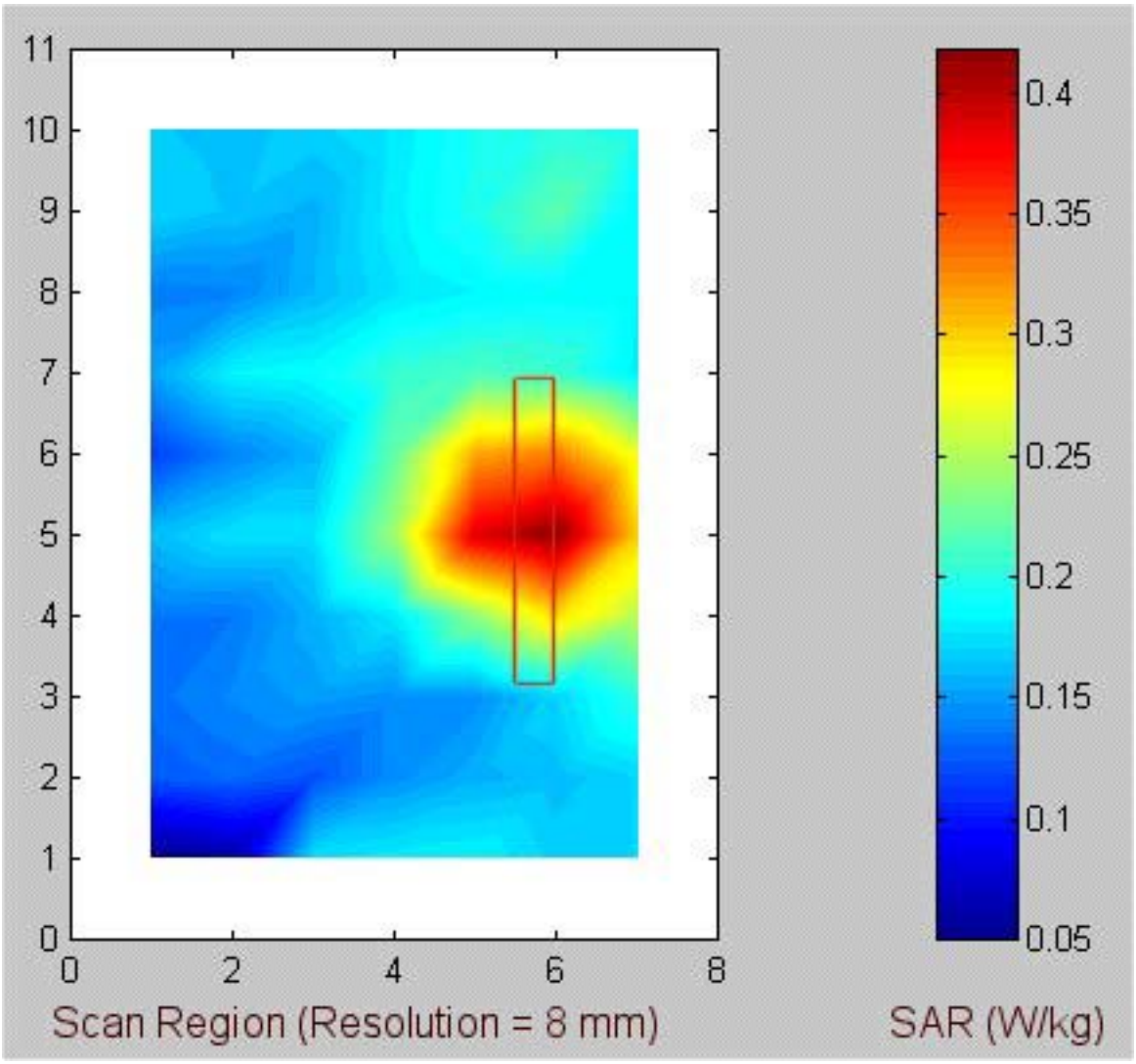

5.25 GHz **Turbo** mode – **Auxiliary** antenna (see Table l for peak 1-g SAR).

Fig. j. Coarse scans for the SAR measurements for the **Edge-on** position of the PC relative to the flat phantom (Configuration 2, see Fig. 4 of the previously submitted SAR report dated February 28, 2003). The right or left edge of the PC with 802.11a Main or Auxiliary antennas, respectively, was placed at 90° at a distance of 1.5 cm from the bottom of the flat phantom.

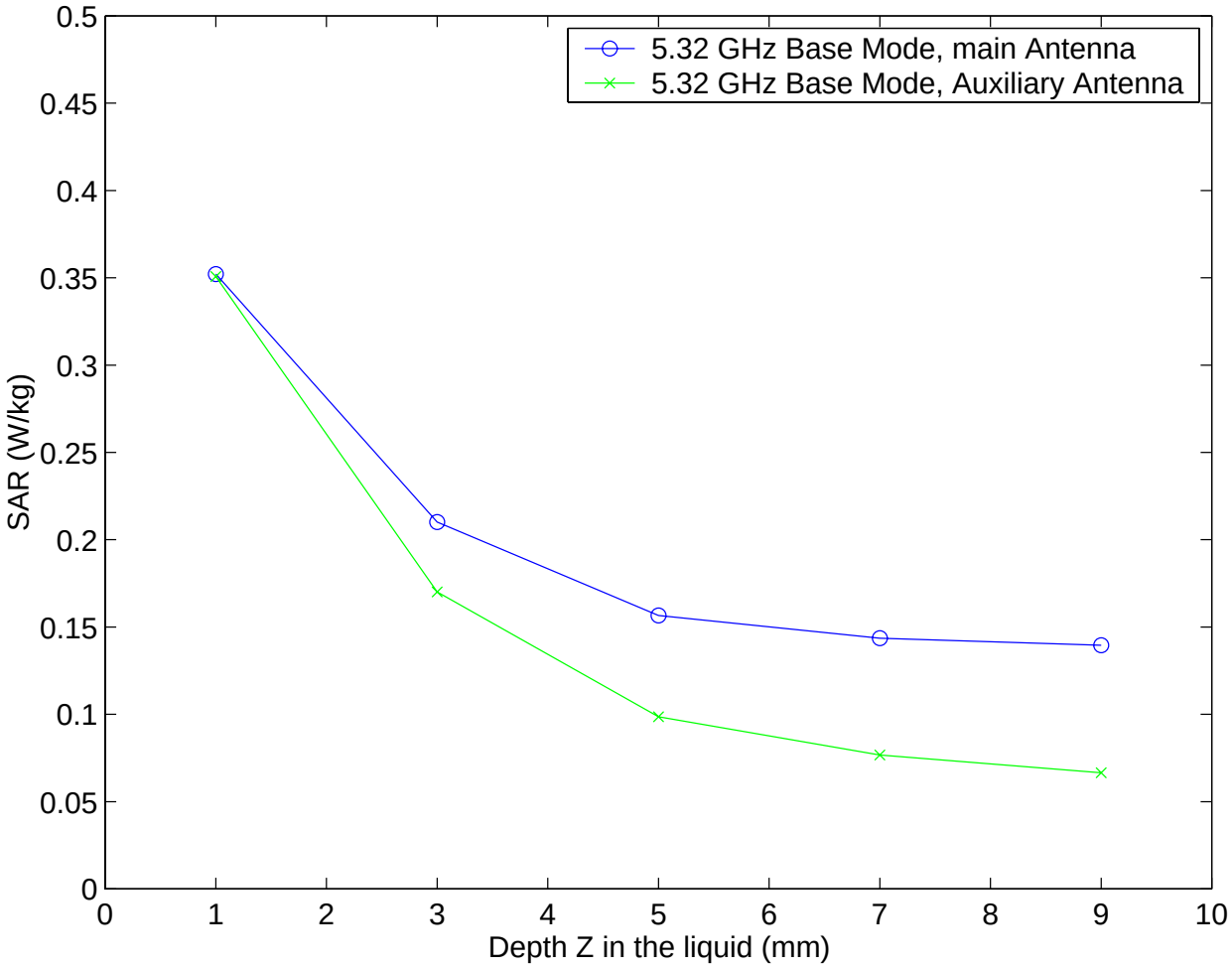

Fig. k. Plot of the SAR variations as a function of depth Z in the liquid for locations of the highest SAR (from Tables c, d for **Configuration 1 – Above-lap position**) for Wistron Neweb EM-500 AG 802.11a Antennas built into Model BQ12 Notebook Computer.

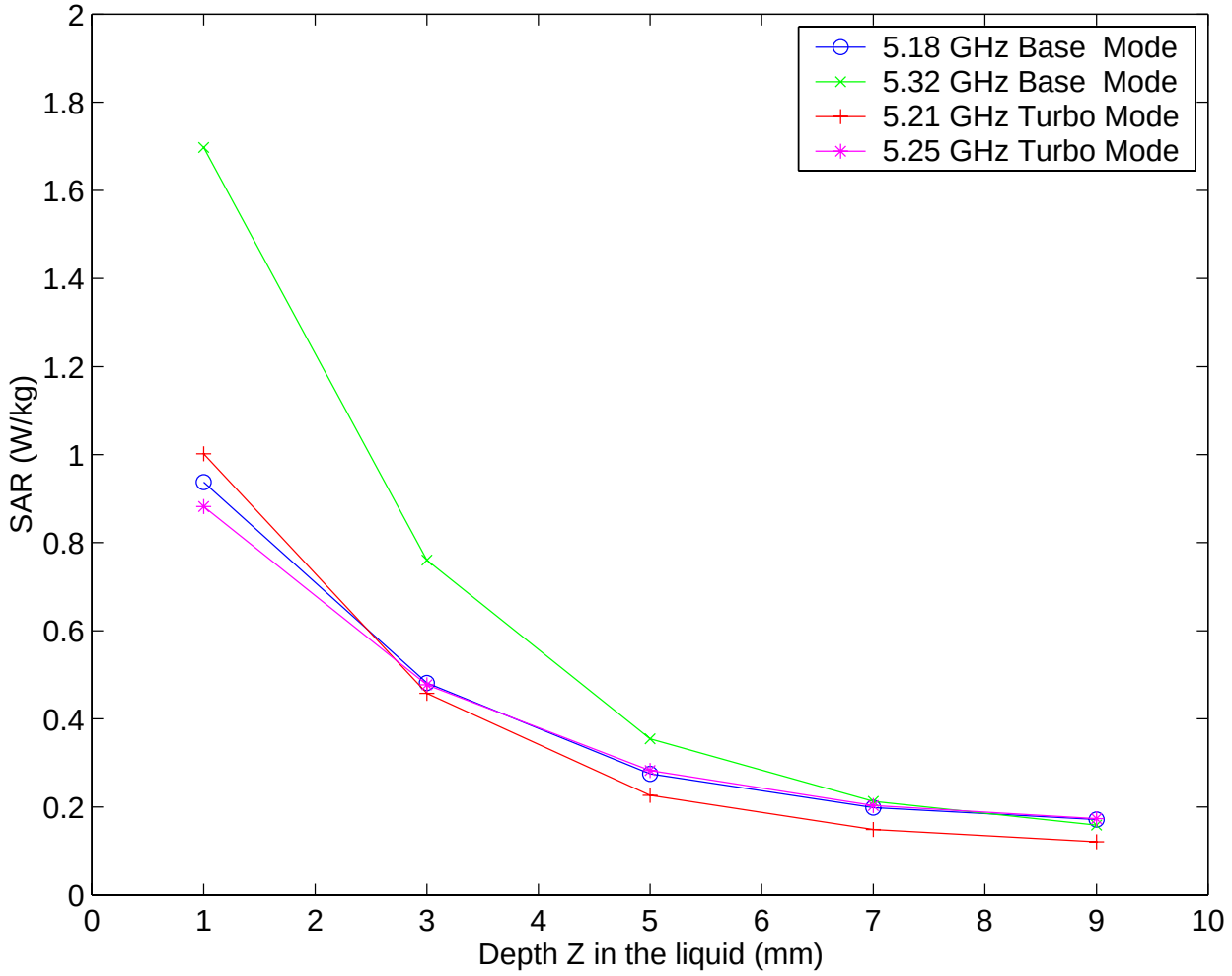

Fig. l. Plot of the SAR variations as a function of depth Z in the liquid for locations of the highest SAR (from Tables e, f for **Configuration 2 – Edge-on position**) for Wistron Neweb EM-500 AG 802.11a **Main** antenna built into Model BQ12 Notebook Computer.

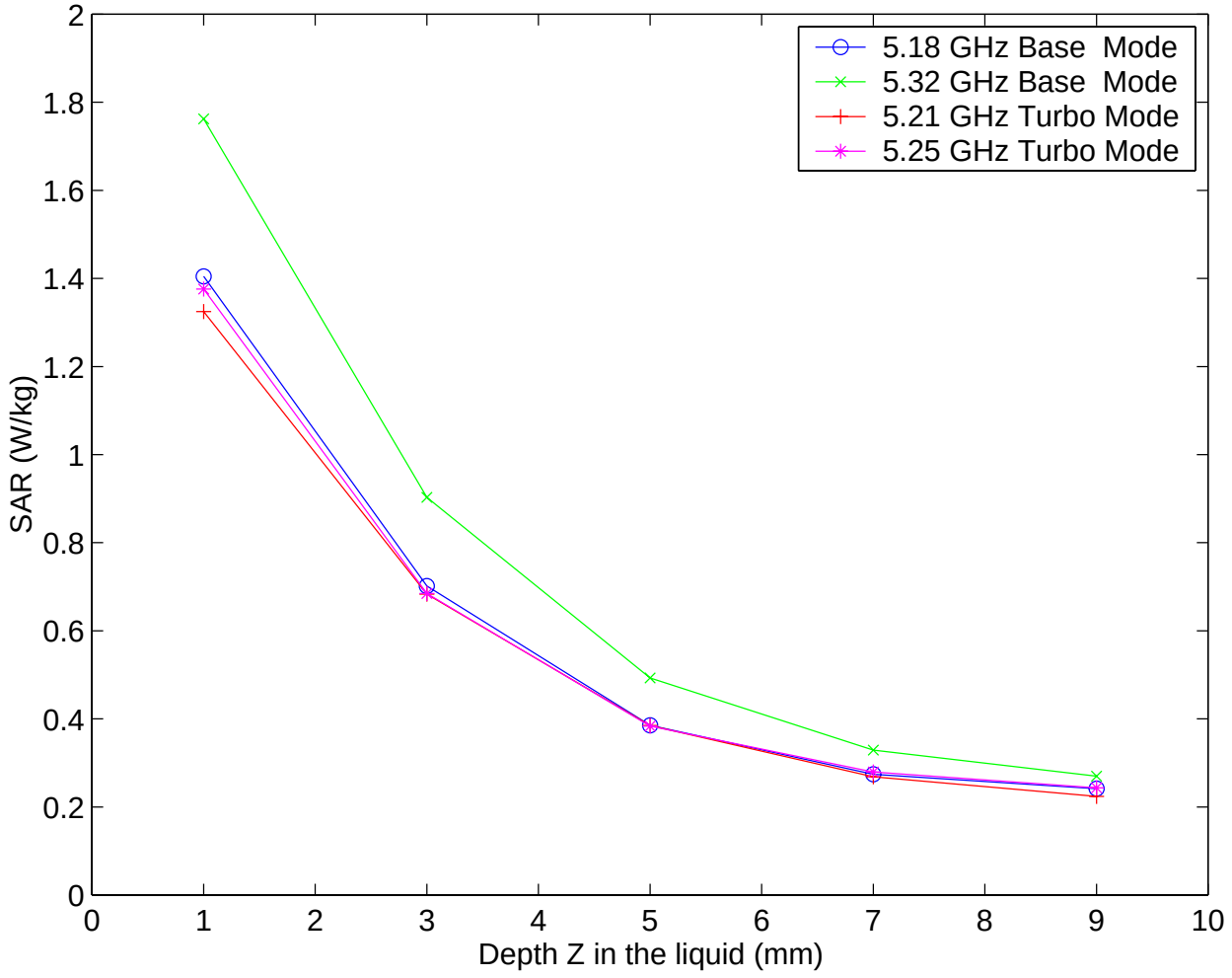

Fig. m. Plot of the SAR variations as a function of depth Z in the liquid for locations of the highest SAR (from Tables e, f for **Configuration 2 – Edge-on position**) for Wistron Neweb EM-500 AG 802.11a **Auxiliary** antenna built into Model BQ12 Notebook Computer.

APPENDIX I

May 6, 2003

AN OPEN-ENDED WAVEGUIDE SYSTEM FOR SYSTEM VALIDATION AND/OR PROBE CALIBRATION IN THE FREQUENCY BAND 5.1 TO 5.8 GHz

Om P. Gandhi
Department of Electrical & Computer Engineering
University of Utah
Salt Lake City, UT 84103

I. Introduction

For frequencies above 800 MHz, the size of a rectangular waveguide is quite manageable and use of an appropriate waveguide filled with a tissue-simulant medium is recommended for calibration of an E-field probe in FCC Supplement C, Edition 01-01 to OET Bulletin 65 [1]. Even though no recommendation is made on choice of an irradiation system for the frequency band 5.1 to 5.8 GHz, balanced half-wave dipoles have been suggested for system validation for frequencies less than or equal to 3000 MHz [1]. It is very difficult to develop half-wave dipole antennas for use in the 5.1 to 5.8 GHz band both because of fairly small dimensions and the resulting dimensional tolerances, and relatively narrow bandwidths of the required baluns – balanced to unbalanced transformers. On the other hand, rectangular waveguides are broadband with simultaneous bandwidths larger than 1-2 GHz and are fairly easy to use for frequencies in excess of 3 GHz. We have, therefore, developed an open-ended waveguide system for SAR system validation and/or probe calibration in the frequency band 5.1 to 5.8 GHz.

II. The Waveguide Irradiation System

We have used a WR187 rectangular waveguide of internal dimensions 1.872" × 0.872". The operating (TE_{10} mode) band of this waveguide is from 3.95 to 5.85 GHz. This is considerably larger than the required bandwidth of 0.7 GHz for the frequency band 5.1 to 5.8

GHz. The waveguide irradiation system used for SAR system validation is shown in Fig. 1. As recommended in [1], the open-ended waveguide irradiator is placed at a distance of 8 mm below the base of planar phantom with inside dimensions 12" × 16.5" (30.5 × 41.9 cm) and a base thickness of 2.0 ± 0.2 mm. This results in the open end of the waveguide at a distance of 10 mm below the lossy fluid in the phantom. The microwave circuit arrangement used for the waveguide irradiation system is shown in Fig. 2. As shown in Fig. 2, the WR187 waveguide is fed with microwave power from a Hewlett Packard Model 83620A Synthesized Sweeper (10 MHz-20 GHz). When placed at a distance of 8 mm below the base of the planar phantom, the reflection coefficient is about 10-20%. Even this relatively small amount of reflection has been greatly reduced to less than 0.5% by using a movable slide-screw waveguide tuner (Narda Model 22CI). The planar phantom is filled to a depth of 15 cm with a fluid to simulate dielectric properties recommended for the body phantom in [1]. The dielectric constants ε_r and conductivities σ at the experimental frequencies of 5.25 and 5.8 GHz are: $\varepsilon_r = 49.0$, $\sigma = 5.30$ S/m at 5.25 GHz; and $\varepsilon_r = 48.2$, $\sigma = 6.00$ S/m at 5.8 GHz.

III. Calculation of the SAR Distributions

We have used the finite-difference time-domain (FDTD) numerical electromagnetic method to calculate the electric fields and SAR distributions for the planar phantom of base thickness 2.0 mm of dielectric constant $\varepsilon_r = 2.56$ and dielectric properties of the tissue-simulant lossy fluid as given in Section II. For the FDTD calculations, we have used a cell size δ = 0.5 mm in order to meet the requirement $\delta \leq \lambda_\varepsilon / 10$ in the lossy fluid. The calculated variations of the SAR distribution at the experimental frequencies of 5.25 and 5.80 GHz are given in Figs. 3 and 4, respectively. Also shown in the same figures are the experimental values of the SARs (shown by red circles) at heights of 4, 6, 8, 10, 12, and 14 mm above the bottom surface of the phantom fluid. From Figs. 3 and 4, it is obvious that the penetration of electromagnetic fields in the 5.1 to 5.8 GHz band is extremely shallow. The calculated depths of penetration corresponding to $1/e^2$-reduction of SAR (13.5% of the SAR at the surface) are only

6.85 and 5.985 mm at 5.25 and 5.8 GHz, respectively. Both of these depths of penetration are very similar to those obtained for plane-wave irradiation at these frequencies (7.15 mm for 5.25 GHz and 6.25 mm for 5.8 GHz).

IV. Need for Extrapolation and Comparison of Measured and Calculated SAR Distribution

Because of the physical separation of the three orthogonal pickup dipoles from the tip of the E-field probe, the SAR measurements cannot be taken any closer than about 3 mm from the bottom surface of the phantom fluid. As given in Figs. 3 and 4, we have measured the SARs with 2 mm resolution at heights of 4, 6, 8, 10, 12 and 14 mm above the bottom surface of the phantom fluid. We have tried second-, third-, fourth-, and fifth-order polynomial least-square fits to extrapolate the measured data to obtain SARs closer to the bottom of the lossy fluid. As seen in Figs. 3 and 4, the second- and third-order polynomials underestimate the SARs while the fifth-order polynomial overestimates the SAR distribution. An excellent least-square fit to the numerically-calculated SAR variations is obtained by using a fourth-order polynomial to extrapolate the measured data both at 5.25 and 5.8 GHz. The coarse scans of the SAR distributions measured with a resolution of 8 mm in the xy plane at a height Z of 4 mm above the bottom surface of the phantom fluid are given in Figs. 5 and 6 for experimental frequencies of 5.25 and 5.8 GHz, respectively. Also shown in these figures is the outline of the open end of the waveguide overlaid on the SAR contours.

After identifying the region of the highest SAR, the SAR distributions were measured with a finer resolution of 2 mm in order to obtain the peak 1 cm^3 or 1-g SAR. Here too, the SAR measurements were performed at 4, 6, 8, 10, 12, and 14 mm height from the bottom surface of the body-simulant fluid. The SARs thus measured were extrapolated using a fourth-order least-square fit to the measured data to obtain values at 1, 3, 5, 7, and 9 mm height and used to obtain peak 1-g SARs. For a radiated power of 100 mW, the SARs thus obtained with 2 mm resolution for xy planes at heights Z of 1, 3, 5, 7, and 9 mm for the peak SAR region of volume 10 ×10 ×

10 mm are given in Tables 1 and 2, respectively. The experimentally-determined peak 1-g SARs for 100 mW of radiated power of 3.678 and 3.947 W/kg are extremely close to the FDTD-calculated 1-g SARs for this waveguide irradiator of 3.580 and 3.946 W/kg at 5.25 and 5.80 GHz, respectively.

V. Conclusions

We have developed an open-ended waveguide irradiation system for validation of the SAR measurement system and/or for E-field probe calibration in the frequency band 5.1 to 5.8 GHz. A fourth-order polynomial least-square fit to the experimental data gives SAR variations close to the bottom surface of the phantom that are in excellent agreement with those obtained using the FDTD method. The experimentally-determined peak 1-g SARs are within 1 to 2 percent of those obtained using the FDTD numerical calculations.

References

1. Federal Communications Commission, "Supplement C Edition 01-01 to OET Bulletin 65 Edition 97-01", June 2001.

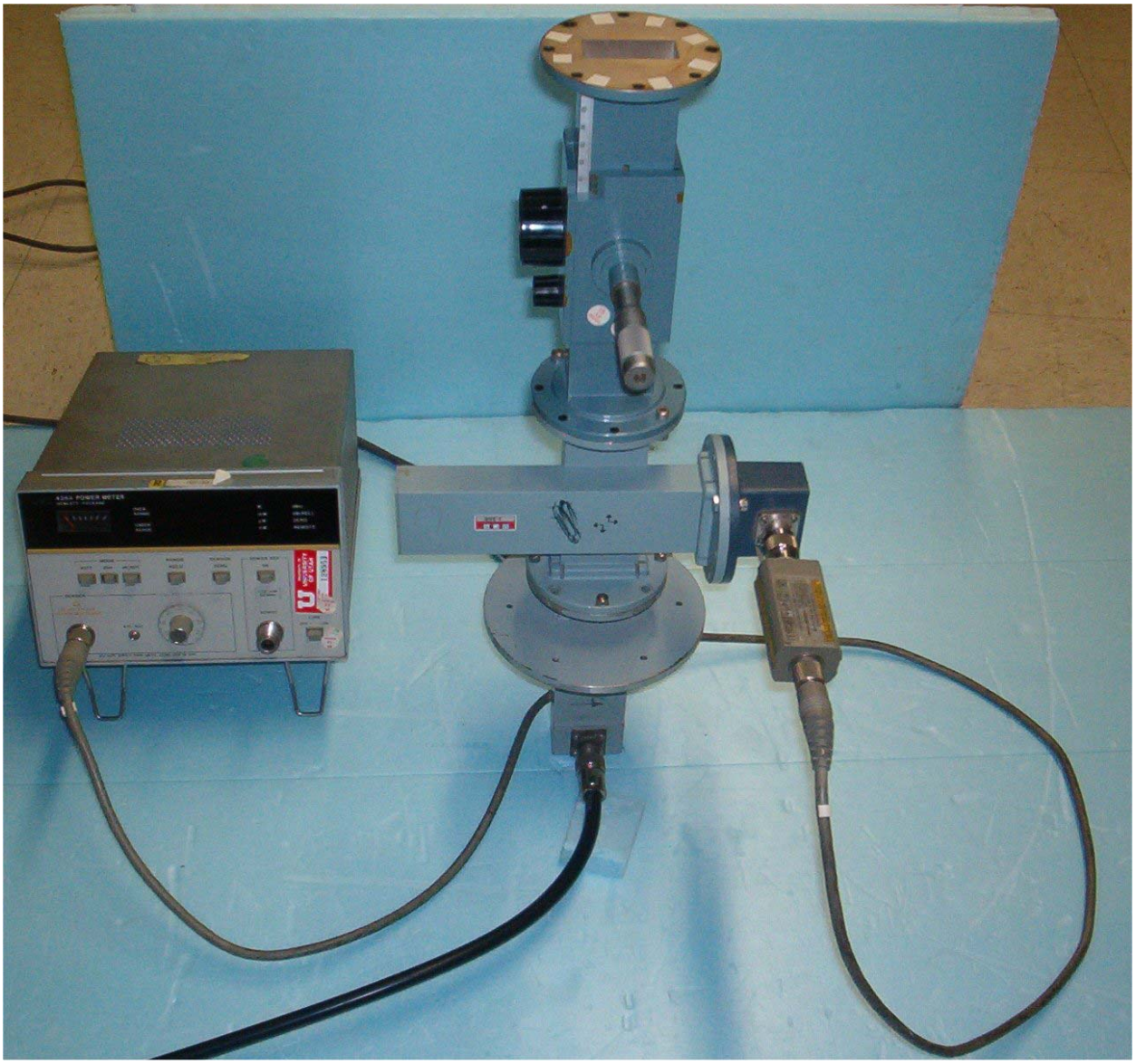

Fig. 1. Photograph of the rectangular waveguide radiator used for system verification. Also seen is the Narda Model 22CI movable slide screw tuner used to match the input power at 5.25 or 5.8 GHz to the planar phantom.

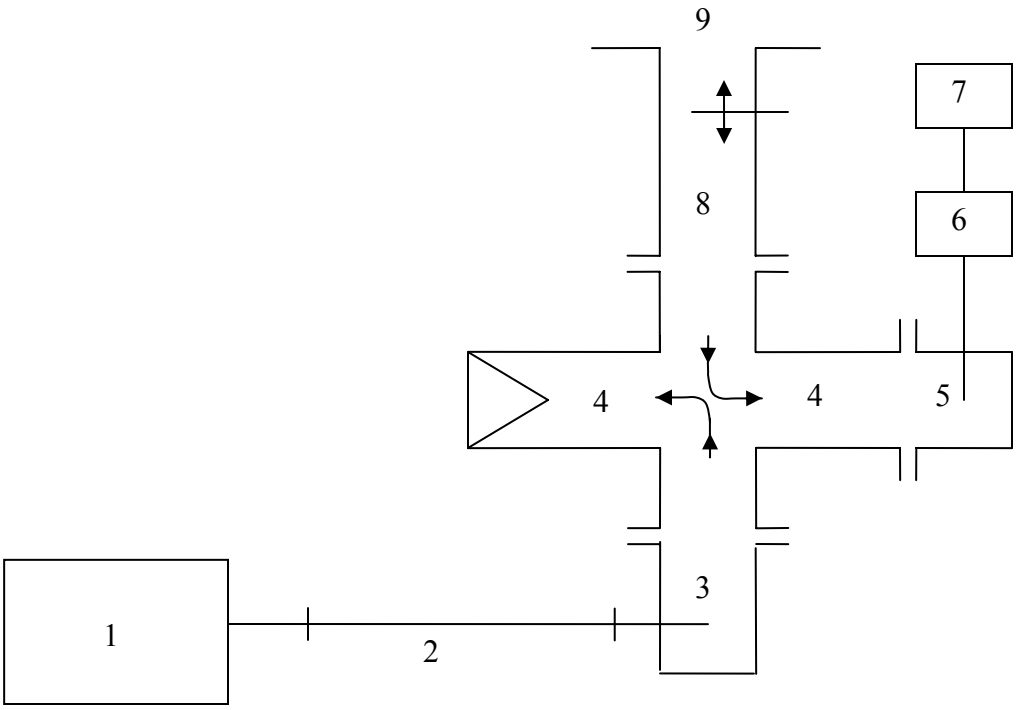

1. Hewlett Packard (HP) Model 83620A Synthesized Sweeper (10 MHz-20 GHz).
2. Coaxial line.
3. Coaxial to waveguide adapter.
4. 20 dB crossguide coupler (may be reversed to measure incident power).
5. HP Model G281A coaxial to waveguide adapter
6. HP Model 8482A power sensor.
7. HP Model 436A power meter.
8. Narda Microline® Slide Screw Tuner Model 22CI.
9. Radiating open end of the waveguide.

Fig. 2. The microwave circuit arrangement used for SAR system verification.

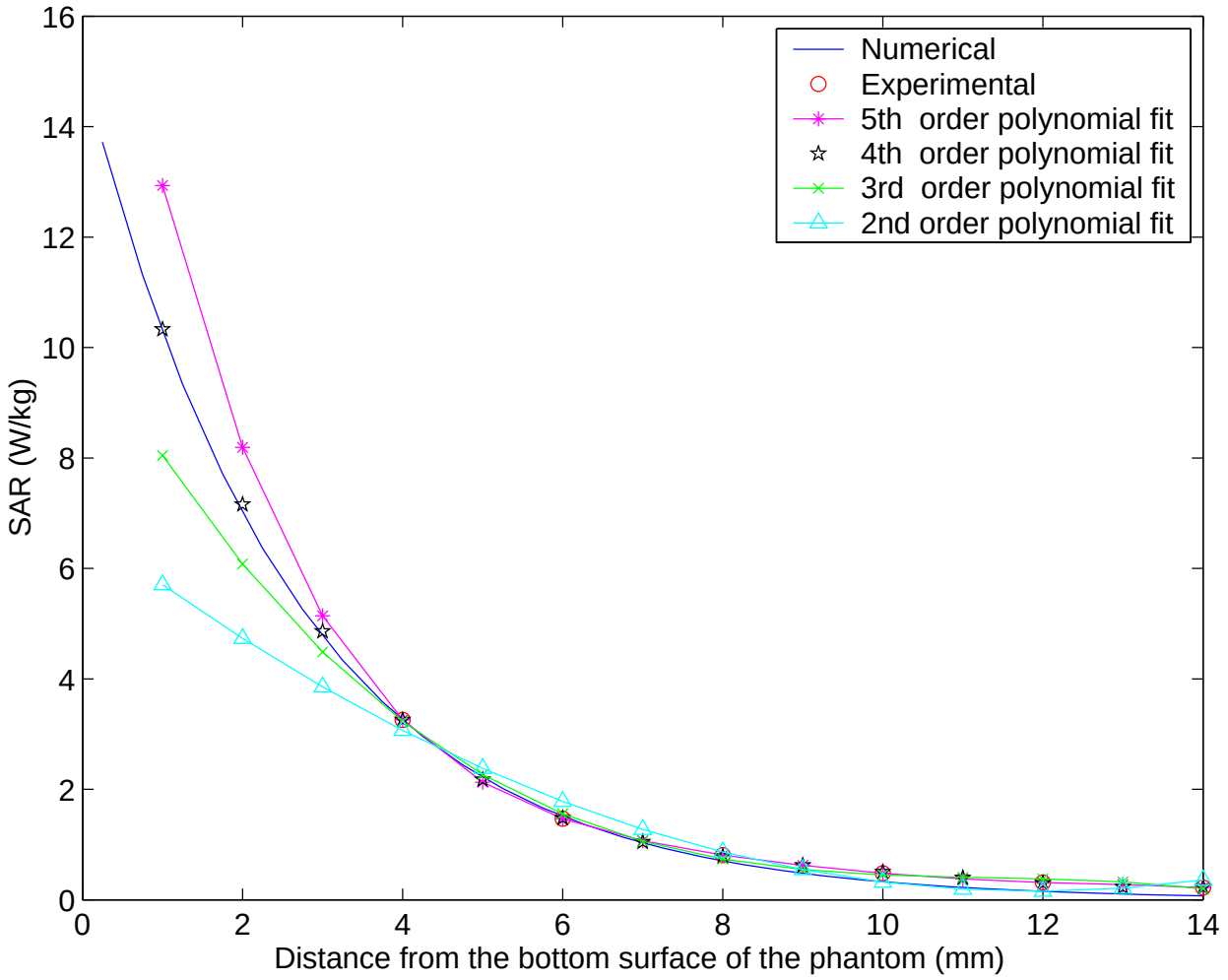

Fig. 3. Comparison of the experimentally measured and FDTD-calculated variation of the SAR with depth in the body-simulant planar phantom at 5.25 GHz. Also shown are the SARs extrapolated from experimental values to heights of 1, 3, 5, 7 and 9 mm above the bottom of the phantom using second-, third-, fourth-, and fifth-order least-square fit polynomials.

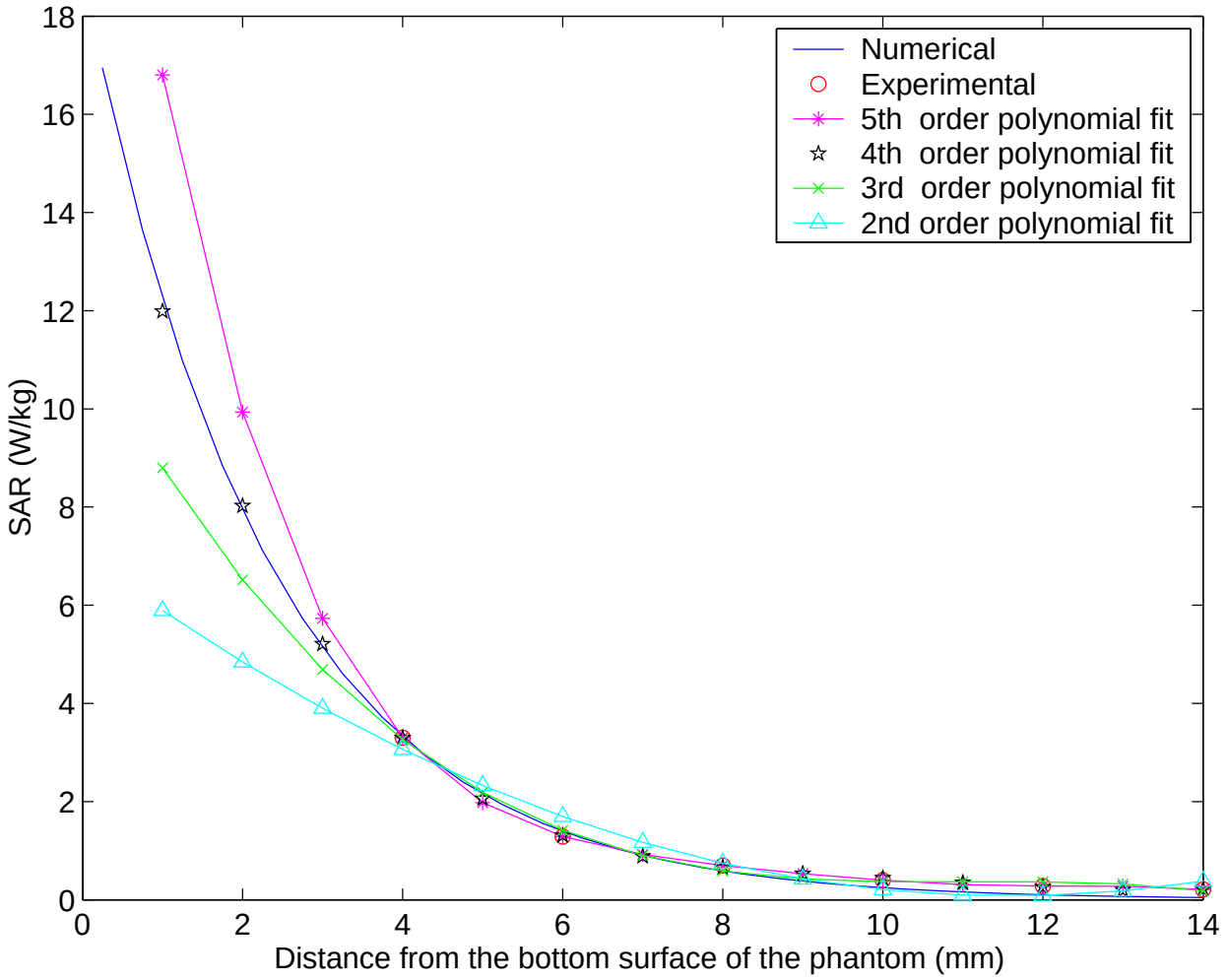

Fig. 4. Comparison of the experimentally measured and FDTD-calculated variation of the SAR with depth in the body-simulant planar phantom at 5.8 GHz. Also shown are the SARs extrapolated from experimental values to heights of 1, 3, 5, 7 and 9 mm above the bottom of the phantom using second-, third-, fourth-, and fifth-order least-square fit polynomials.

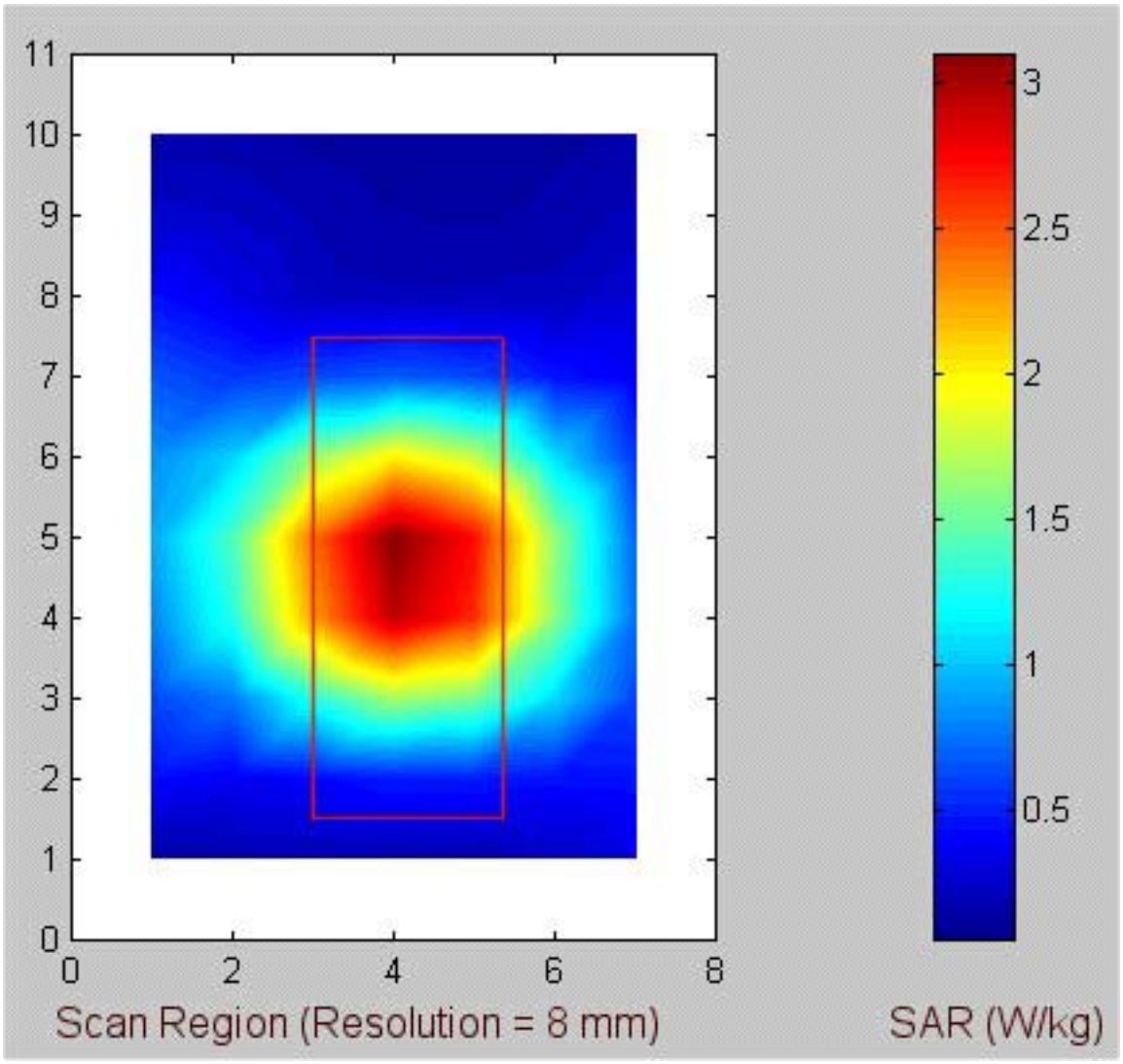

Fig. 5. Coarse scans of the measured SAR distribution for the WR187 rectangular waveguide irradiation system used for system verification at 5.25 GHz. Radiated power = 100 mW.

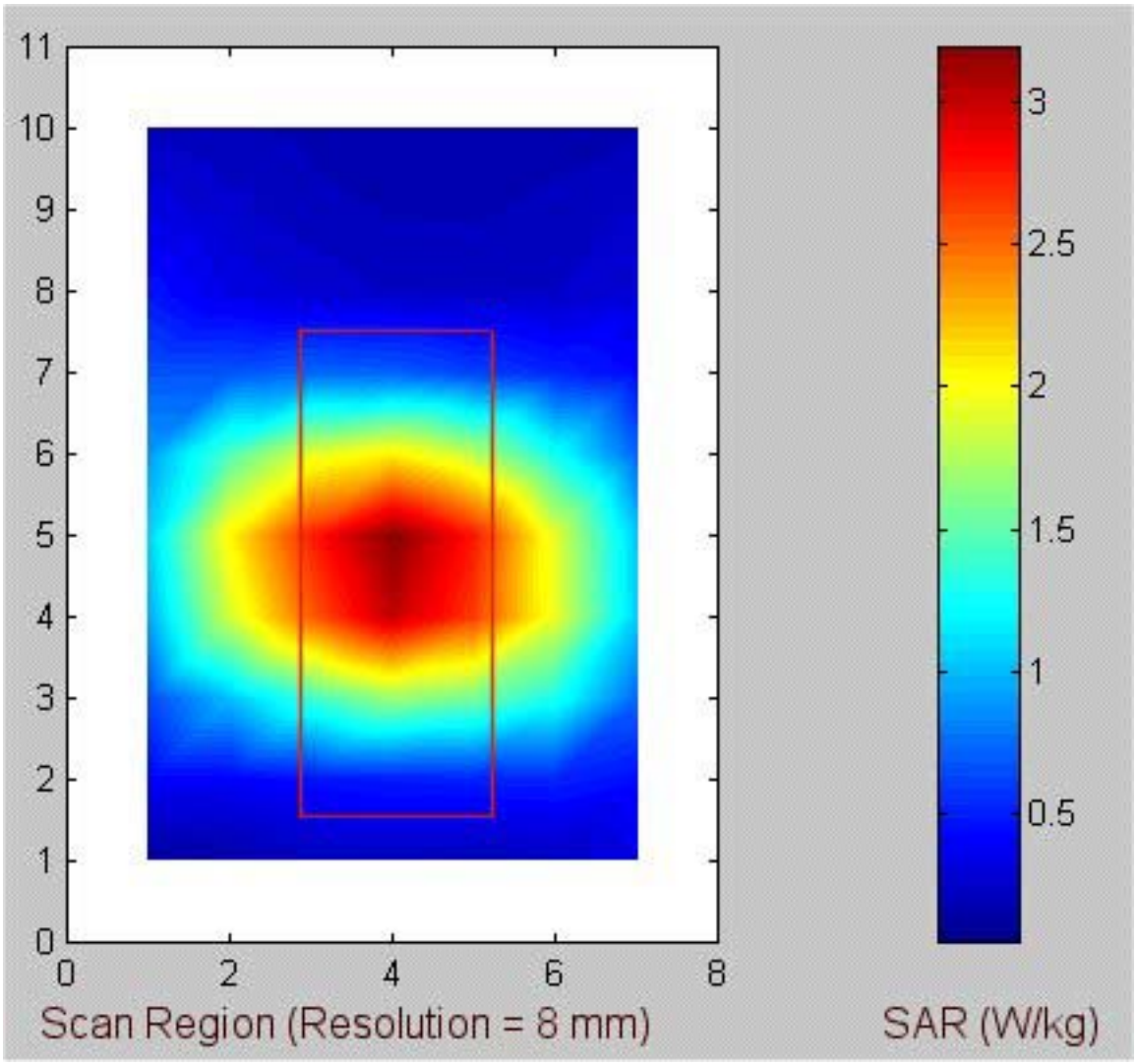

Fig. 6. Coarse scans of the measured SAR distribution for the WR187 rectangular waveguide irradiation system used for system verification at 5.8 GHz. Radiated power = 100 mW.

Table 1. The SARs measured and extrapolated for the WR187 open-ended waveguide placed below the planar phantom at a distance of 10 mm below the bottom surface of the tissue-simulant fluid. Radiated power = 100 mW, frequency = 5.25 GHz.

1-g SAR = 3.678 W/kg

a. At depth of 1 mm

9.201	9.627	9.989	9.919	9.628
9.790	10.137	10.522	10.397	10.063
10.067	10.674	10.708	10.714	10.371
9.933	10.428	10.709	10.715	10.317
9.762	10.192	10.328	10.284	9.917

b. At depth of 3 mm

4.199	4.390	4.528	4.528	4.421
4.457	4.643	4.786	4.760	4.636
4.595	4.846	4.884	4.899	4.769
4.561	4.758	4.890	4.893	4.735
4.457	4.645	4.731	4.719	4.575

c. At depth of 5 mm

1.822	1.903	1.943	1.969	1.925
1.923	2.013	2.068	2.066	2.029
1.983	2.086	2.113	2.123	2.076
1.978	2.052	2.116	2.113	2.058
1.931	2.002	2.061	2.063	2.006

d. At depth of 7 mm

0.878	0.916	0.923	0.950	0.920
0.916	0.960	0.988	0.986	0.972
0.939	0.998	1.009	1.010	0.987
0.936	0.973	1.007	1.000	0.979
0.926	0.953	0.993	0.997	0.968

e. At depth of 9 mm

0.539	0.560	0.558	0.581	0.554
0.555	0.583	0.594	0.595	0.583
0.565	0.610	0.612	0.604	0.590
0.559	0.590	0.604	0.595	0.586
0.568	0.586	0.604	0.604	0.593

Table 2. The SARs measured and extrapolated for the WR187 open-ended waveguide placed below the planar phantom at a distance of 10 mm below the bottom surface of the tissue-simulant fluid. Radiated power = 100 mW, frequency = 5.8 GHz.

1-g SAR = 3.947 W/kg

a. At depth of 1 mm

10.705	11.116	11.054	11.024	10.620
11.337	11.704	11.800	11.627	10.982
11.543	11.928	11.988	11.877	11.132
11.653	12.027	11.862	11.680	11.311
11.212	11.550	11.669	11.304	10.889

b. At depth of 3 mm

4.677	4.814	4.821	4.794	4.649
4.908	5.072	5.128	5.020	4.795
5.001	5.173	5.211	5.129	4.899
5.032	5.180	5.182	5.072	4.905
4.848	4.983	5.030	4.906	4.729

c. At depth of 5 mm

1.885	1.910	1.931	1.911	1.870
1.945	2.006	2.041	1.980	1.928
1.979	2.044	2.061	2.022	1.971
1.985	2.035	2.064	2.007	1.945
1.916	1.969	1.983	1.951	1.886

d. At depth of 7 mm

0.845	0.840	0.855	0.841	0.826
0.851	0.873	0.890	0.859	0.856
0.862	0.882	0.884	0.874	0.857
0.867	0.879	0.889	0.864	0.849
0.835	0.864	0.864	0.857	0.834

e. At depth of 9 mm

0.528	0.521	0.531	0.518	0.504
0.520	0.538	0.535	0.520	0.524
0.525	0.534	0.530	0.523	0.514
0.538	0.527	0.529	0.517	0.519
0.511	0.532	0.526	0.528	0.516

APPENDIX II

SAR System Verification for May 22, 2003

The measured SAR distribution for the peak 1-g SAR region using
WR187 rectangular waveguide irradiation system

For May 22, 2003 – The SAR plot at 5.25 GHz

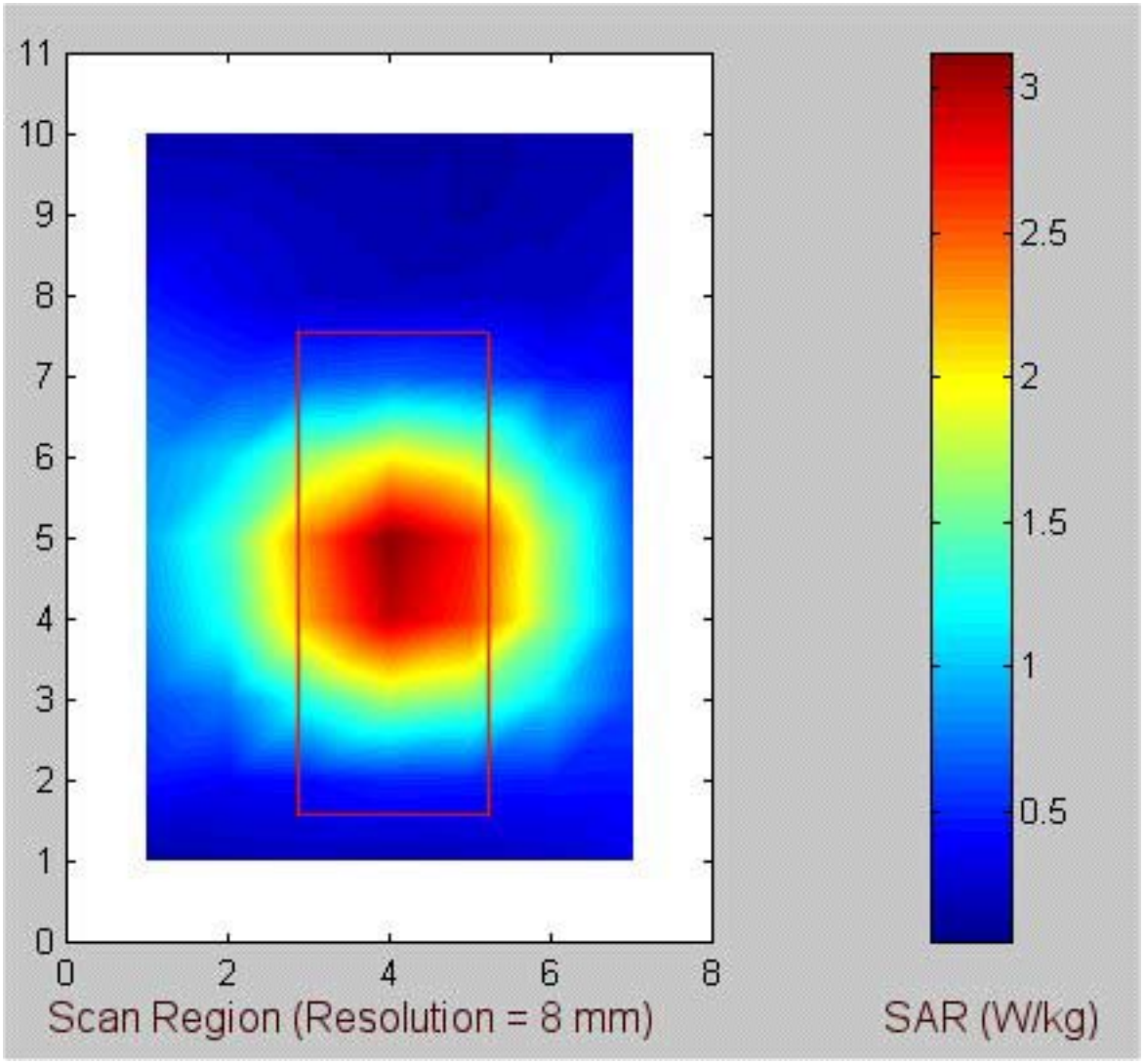

Fig. II.1. Coarse scans of the measured SAR distribution for the WR187 rectangular waveguide irradiation system used for system verification at 5.25 GHz. Also shown is the outline of the rectangular waveguide overlaid on the SAR contours. Radiated power = 100 mW.

1-g SAR = 3.665 W/kg

a. At depth of 1 mm

9.099	9.634	10.044	9.882	9.474
9.812	10.141	10.364	10.400	9.967
10.030	10.726	10.725	10.665	10.307
9.914	10.321	10.625	10.751	10.277
9.658	10.231	10.322	10.221	9.838

b. At depth of 3 mm

4.166	4.376	4.518	4.516	4.381
4.454	4.637	4.745	4.754	4.604
4.581	4.834	4.878	4.871	4.739
4.541	4.722	4.867	4.889	4.721
4.423	4.633	4.711	4.689	4.545

c. At depth of 5 mm

1.818	1.891	1.930	1.962	1.921
1.915	2.005	2.063	2.057	2.022
1.980	2.072	2.104	2.115	2.069
1.967	2.047	2.114	2.103	2.051
1.926	1.988	2.050	2.056	1.996

d. At depth of 7 mm

0.882	0.912	0.923	0.944	0.920
0.911	0.954	0.988	0.980	0.973
0.939	0.997	1.004	1.014	0.991
0.934	0.977	1.006	0.997	0.972
0.930	0.953	0.992	1.001	0.966

e. At depth of 9 mm

0.544	0.562	0.565	0.577	0.555
0.552	0.580	0.594	0.596	0.584
0.566	0.617	0.609	0.609	0.596
0.565	0.595	0.600	0.601	0.583
0.574	0.593	0.606	0.610	0.594